ANODIZED ALUMINA AS A TEMPLATE FOR NANOSTRUCTURE PROCESSING

by

Alain Gabriel Mbengu Kassangana

Department of Mining and Metallurgical Engineering,

McGill University

Montreal, Canada

June 2007

A thesis submitted in partial fulfillment of the

requirements for the degree of

Master's of Engineering

McGill University

Your file Votre référence
ISBN: 978-0-494-51462-7
Our file Notre référence
ISBN: 978-0-494-51462-7

ABSTRACT

A novel way of producing nanostructures in the past decade has been through the use of an anodized alumina template. This template has dense, self-ordered nanometric pores that grow in the oxide as the aluminum is being anodized. This technique is a fairly new method of processing nanostructures, and much study and research is presently being done to understand the formation mechanisms of the highly ordered pores. Ultra-pure aluminium foil and pure aluminium single crystal plates were anodized to create porous anodized alumina, and using it as a template to electro-deposit Nickel nanostructures. The effects different anodizing parameters have on oxide creation were studied, and the results obtained from studying the effects of substrate purity and texture of the anodized aluminum substrate on the morphology of the alumina template, through the use of X-ray diffraction and scanning electron microscopy.

Nickel nanowires were prepared by DC electrodeposition inside the porous alumina template with a gold-palladium coating serving a conductive base. The nanowires have a diameter of 65 nm, and their length depends on the deposition time. The nanowires can uphold a position perpendicular to the substrate by partially dissolving the alumina template. They also have a tendency to gather together once the template is partially removed.

RESUMÉ

Une nouvelle façon de reproduire des nanostructures consiste a créer ces nanostructure la déposition électrolytique dans un calibre d'alumine anodisé. Le calibre comporte des pores nanometric denses et très ordonnés qui se développent pendant que l'aluminium est anodisé. Cette technique est une méthode assez nouvelle de façonner des nanostructures, et de nombreuses études et recherches se font actuellement pour comprendre les mécanismes de formation de ces pores fortement ordonnées. Du papier d'aluminium ultra-pur et les plaque purs d'aluminium ont été anodisés pour créer l'alumine poreuse, et elle a été employée comme calibre pour l'électrodéposition des nanostructures de nickel. Les effets des différents paramètres d'anodisation, soit les effets de la pureté et de la texture du substrat en aluminium sur la morphologie du calibre d'alumine, ont été analysé par la microscopie électronique a balayage et la diffraction de rayon X.

Des nanofils de nickel ont été fabrique par la déposition électrolytique à l'intérieur du calibre poreux d'alumine avec un or-palladium enduit servant de base conductrice. Les nanofils ont un diamètre de 65 nanomètres, et leur longueur dépend du temps de déposition. Les nanofils peuvent maintenir une position perpendiculaire au substrat après la dissolution partiel du calibre d'alumine. Ils ont également une tendance de se recueillir ensemble une fois que le calibre est partiellement enlevé.

ACKNOWLEDGEMENTS

I would first like to thank my thesis supervisor Doctor J.A. Szpunar for his extensive knowledge he shared with me. His vision and desire for novel discoveries and research result in high expectations from his students. For his kindness, patience and motivation I am forever thankful.

I would also like to extend my gratitude to the whole texture and microstructure team of researchers. Roy, Hualong, Marwan, Vladimir, Shahab, Emilie, Jaesoo, Jianlong, Cheol, Kabir, Andy, Tedric, Raman, and everyone else, thank-you very much for your help, support and advise throughout my time at McGill. You made it very easy for me to learn how to use the equipment in the laboratory. Special thanks goes out to Slavek Poplawski, our devoted laboratory technician for conveying his expertise, keeping the equipment running, and also for his sense of humour which more than once kept my day animated.

TABLE OF CONTENTS

LIST OF FIGURES

LIST OF TABLES

CHAPTER 1: INTRODUCTION

With today's scientific advancement, technology is being extremely minimized, not by its importance, but by its size. Indeed it seems as though every cell phone, digital camera, or any other electronic device is getting smaller, but more enhanced none the less. The new and innovative approach of storing more information in smaller devices is being heavily sought and researched. Nanotechnology is the science of manipulating materials on an atomic scale. In such, nanotechnology is the means of making smaller, more performing devices, and it has become a subject of much concern, exhaustive research and even profitable ventures. Since miniaturization is the central idea of modern fabrication technology, nanotechnology has been taking the industry by storm.

Nevertheless, the nanotechnology route has been taken long before it actually became trendy, and is still a new and natural step towards the evolution of microelectronics. It presents an access to a new concept in engineering, due to the fact that nano-scale is comparable to the electron wavelength (depending on its wavelength), and the size of biological molecules.

Nanotechnology can best be thought of as a description of activities at the level of atoms and molecules used in real world applications. A nanometre is a billionth of a meter, that is, about 10 times the diameter of a hydrogen atom. It includes precision engineering along with electronics, mechanical systems, as well as conventional biomedical applications in areas ranging from gene therapy to drug delivery and innovative drug discovery methods [1, 2].

There are two fundamentally different approaches to nanotechnology, which are termed 'top down' and 'bottom up'. 'Top-down' refers to making nanoscale structures by machining and etching techniques, whereas 'bottom-up', also called molecular

nanotechnology, is used to describe building structures atom-by-atom, or molecule-by-molecule. Top-down or bottom-up illustrates a measure of the amount of progress of nanotechnology. Nanotechnology, as it is applied today, can still be regarded as at more primitive 'top-down' stage [2].

Another characteristic of nanotechnology is that it is an area of research and development that is truly multidisciplinary. Nano-scale research is combined by the need to share new knowledge on techniques, as well as information on the physics affecting both the atomic and molecular interactions in the field. Materials scientists, mechanical and electronic engineers and medical researchers join with biologists, physicists and chemists in order to get an even broader understanding of how the use of such a technology can affect today's society.

With nanotechnology's great potential also come social and ethical issues. These issues include environmental and health issues, privacy issues, and other more ethical issues, just to name a few examples. Environmentally speaking, nanotechnology followers argue that making things much smaller reduce energy demands, and will make them more energy efficient, which in a sense is the driving force of research projects such as this one.

Like any other new field, nanotechnology does bring uncertainty in what the future might hold for society. Nevertheless, it is a very promising field of research and development that will surely bring much advancement in the medical, physical and chemical engineering realms.

This thesis will focus on a method of synthesising nanostructures through an anodized alumina template. First, the process of anodizing alumina and the resulting effect will be treated. This will be followed by the synthesis of nickel nanowires through the use of the anodized template. The specific objectives of the research were:

1- Determining the appropriate anodizing conditions with regards to anodizing time, and aluminium surface preparation.

2- Examining the effects of aluminium purity on the anodized alumina

3- Determining the effects of texture, grain size and grain boundaries on the anodized alumina

4- Synthesizing Nickel nanostructures through electrodeposition process with a Watts Nickel deposition bath.

The sequence in which the different chapters appear in this paper follow the chronological order of the research performed. This work also comprises a literature review (chapter 2) of previous accumulated knowledge and research done on anodized alumina and nanostructure processing using the anodized alumina template. The section also compares the lithography approach of nanostructure processing with the template assisted method. The following chapter explains the procedures of anodizing, and the optimal anodizing conditions are adopted after a sequence of trial and error anodizing experiments. The influence of purity, grain size and grain boundary on the structure of the anodized alumina template Chapter 4 examines the effects of texture on the morphology and structure of anodized alumina. To facilitate the understanding of the research objectives of the section, a through introduction and explanation of texture and texture measurement is given. Chapter 5, the last chapter dedicated to the accomplished research of this project, will cover the nanostructure deposition process. Again, an ideal settings of deposition current was adopted after a series of trial and error experiments. The last section of this essay will comprise a conclusion, a summary, as well as brief suggestions of future work which should be undertaken in order to achieve all the more substantial results in the field of template deposited nanostructure synthesis.

CHAPTER 2: LITERATURE REVIEW

This chapter present a review of literature about past and present research relevant to anodized aluminium oxide and its use as a template for nanostructure processing. The first part of the chapter includes an introduction to nanotechnology and current methods of producing nanostructures. The second section provides background on the science behind anodizing aluminium. In this section, the theoretical disposition of the experiment and the expected results are discussed. The last section discusses the different kinds of nanostructures obtained through template deposition, as well as data relating to the subject matter accumulated by other researchers.

2.1 NANOTECHNOLOGY

Two hundred years ago, English chemist John Dalton was the first to suggest the scientific theory of the atom. Ever since, chemists have come to understand the elements and atomic interactions, engineers have improved our lives through new and enhanced materials, physicists have unleashed the power of the atomic nucleus, proving that scientific advancement can be detrimental to some, and a source of social and political supremacy for others. In the last two centuries, we have gathered a vast understanding and now have an increasing control over the fundamental unit of matter.

Credit for inspiring nanotechnology usually goes to a brilliant Caltech physicist named Richard Phillips Feynman. In late 1959, Feynman delivered an after-dinner lecture at the annual meeting of the American Physical Society. In that talk, entitled "There's Plenty of Room at the Bottom," Feynman elaborated on work in a field "in which little has been done, but in which an enormous amount can be done in principle"[1]. He lectured about manipulating and controlling things on a small scale, and about miniaturizing without the loss of resolution. He deliberated the possibility of writing the whole encyclopedia on the head of a pin, and gathering all the books on the world to fit on a pamphlet. And yet, it was possible to get smaller still: if all the world's books were converted into an efficient computer code instead of just reduced pictures, you could store all the information that accumulated in all those books in a 'cube of material the size of the barest piece of dust visible to the human eye'. Feynman saw atomic manipulation not only as possible, but inevitable as he boldly declared that the principles of physics, did not go against the possibility of manoeuvring things on an atomic level, and that such development "cannot be avoided".

With the arrival of the scanning tunnelling microscope in 1981, scientists gained a new tool powerful enough see single atoms with unprecedented clarity. This device uses a

tiny electric current and a very fine needle to detect the height of individual atoms. Once scientists discovered that the scanning tunnelling microscope could also be used to precisely pick up and place atoms, one at a time and researchers learned how to rearrange what they saw with the powerful microscope. The first spectacular exhibition of this power came in 1990 when a team of IBM physicists revealed that they had, the year before, spelled out the letters "IBM" using 35 individual atoms of xenon. In 1991, the same research team built an "atomic switch," an important step in the development of nanoscale computing [1].

Another breakthrough came with the discovery of new shapes for molecules of carbon, the quintessential element of life. In 1985, researchers reported the discovery of the "buckyball," a lovely round molecule consisting of 60 carbon atoms. This led in turn to the 1991 discovery of a related molecular shape known as the "carbon nanotube"; these nanotubes are about 100 times stronger than steel but just a sixth of the weight, and they have unusual heat and conductivity characteristics that guarantee they will be important to high technology in the coming years.

2.2 NANOSTRUCTURE PROCESSING METHODS

2.2.1 Electron beam lithography

Nanotechnology is the relatively new science of processing microscopic materials or structures. These nano-sized structures, or nanostructures, are not easily achievable, as one can imagine, because of their extremely small size. However, it is possible to process different types of nanostructures using two different methods. One currently used method is through ion-beam or electron beam lithography, while another consists of using anodized aluminium oxide as a template to "grow" these structures. The lithography method is a less recent technique, and is a much more complex and expensive method than the latter.

Essentially, lithography is the process of transferring patterns from one medium to another. Electron beam lithography (EBL) is a technique for creating extremely fine patterns (0.1um and below) for integrated circuits [6]. This is possible due to the very small spot size of electrons. The electron beam has a very small wavelength, as well as the benefit of extremely high resolution and has been used for transferring patterns having nanometer feature sizes [6, 7].

Nano-scale lithography represents different methods of that originated from the semiconductor industry. It removes or adds material on a substrate, and can be compared to adding bricks or digging holes to construct a building. There are two different methods used in EBL; projection printing, and direct writing, both of which are shown in figure 2.2.1. In projection printing, a large electron beam pattern is projected through the mask onto a substrate by the means of an extremely precise system lenses. Direct writing is the more frequently used of both EBL approaches. In this method, no mask is used, and a beam directly writes on substrate coated with a resist. A lift-off process is commonly used along with direct writing. This process consists of 4 different steps; e-beam resist coating, exposure, development and lift-off. Figure 2.2 shows the process each step at a time.

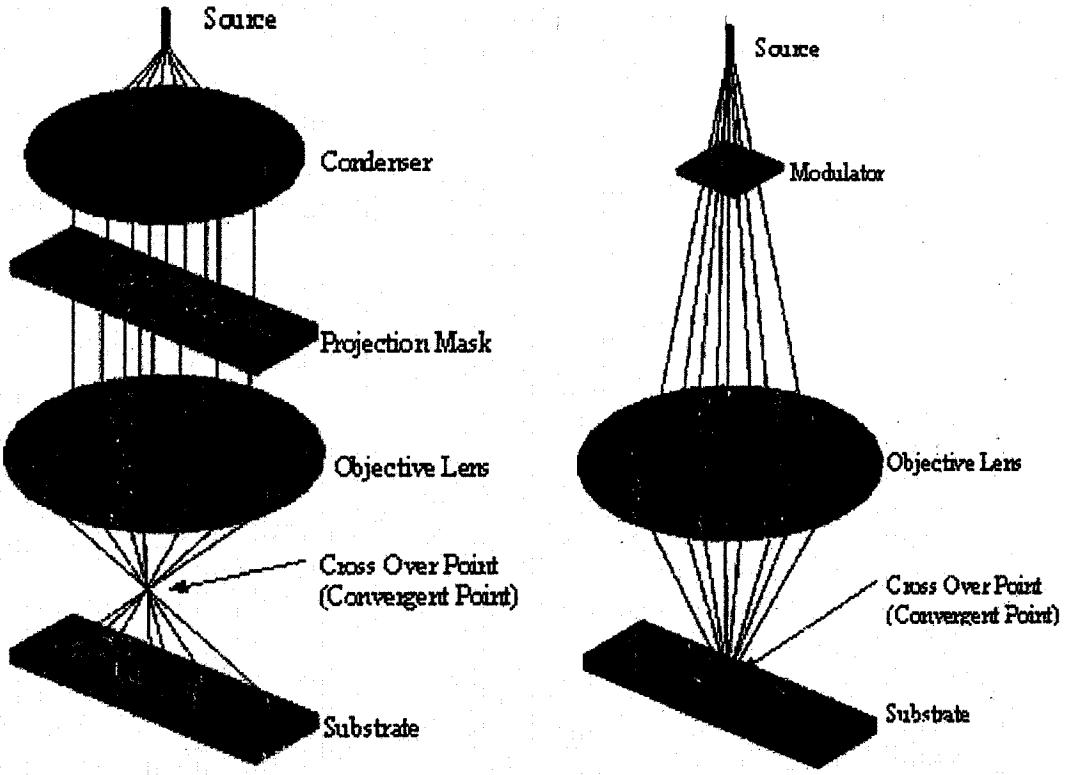

2.2.1

Figure 2.1: Image showing both projection printing (left) and direct writing (right) [7]

Direct writing systems consists of an electron source, a focusing optics set, beam deflection system, and a stage to hold the substrate, basically as shown in figure 2.1. When combined with etching and lifting techniques, it is possible to obtain critical dimensions of 10 nm in the fabrication of electronic devices [8]. Since it is capable of superior resolution without the need for expensive projection optics or time consuming masks production, it has been the most desirable process for nano-fabrication [7]. However, direct writing can only transfer a pattern by exposing one pixel or element at a time, which is very time consuming and expensive when producing a large arrays of nanostructures. Therefore, the limitation caused by the failure of rapid exposure has restricted the use of this technology to only a supporting task in the semiconductor domain.

A much faster and much cheaper method that has been recently developed is the use of anodized porous alumina as a template to grow nanostructure such as nanowires, nanotubes and nanodots. This method, being the main focus of this project, is a promising alternative to both methods described previously for the sole purpose of growing the nanostructures described above.

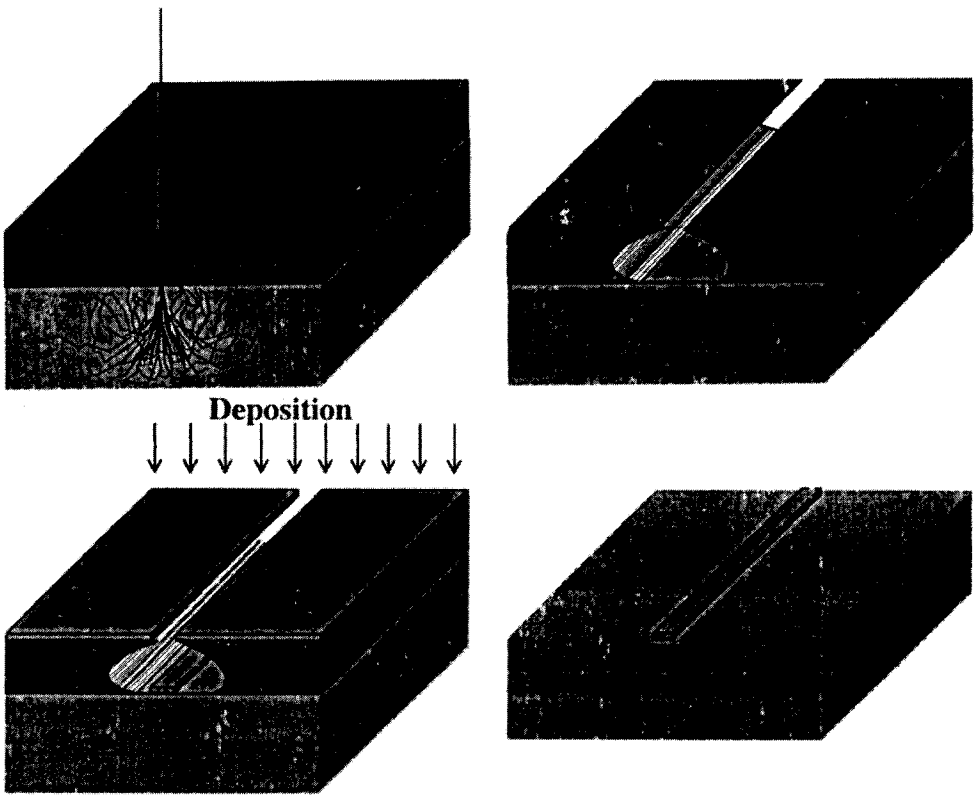

Figure 2.2: Schematic of lift-off process used along with EBL: (a) electron beam is injected, and scattering occurs; (b) exposed resist is removed(c) deposition of desired material by electron gun or vacuum evaporation; (d) lift-off of the unwanted material [6].

2.2.2 Anodized Aluminium template

An oxide film can be grown on certain metals such as aluminium, niobium, tantalum, titanium, tungsten, zirconium through an electrochemical process called anodizing. Depending on the metal, there are anodizing conditions which promote the development of a thin barrier oxide of uniform thickness. The thickness and properties of this layer depend

greatly on the metal, with only the aluminium and tantalum films being of considerable commercial and technological importance as capacitor dielectrics [11]. Aluminium is unique among these metals during anodizing. In addition to the thin barrier of oxide, anodizing aluminium in certain acidic electrolytes produces a thick oxide coating, containing dense microscopic pores. This coating has many important applications including architectural finishes, prevention of corrosion of automobile and aerospace structures, and electrical insulation [11].

The latest study in nanostructure processing also includes the use of anodized aluminium oxide. The reason this ceramic is heavily being studied is due to its morphology, its stability at high temperatures, and its inertness. The anodizing process attained by establishing an electrical circuit between a cathode and the aluminium substrate (serving as an anode) through an acidic electrolyte (figure 3). The anodic alumina grows as a very uniform porous array, with hexagonal packing. Since this represents the highest packing factor, the porous array is as dense as possible.

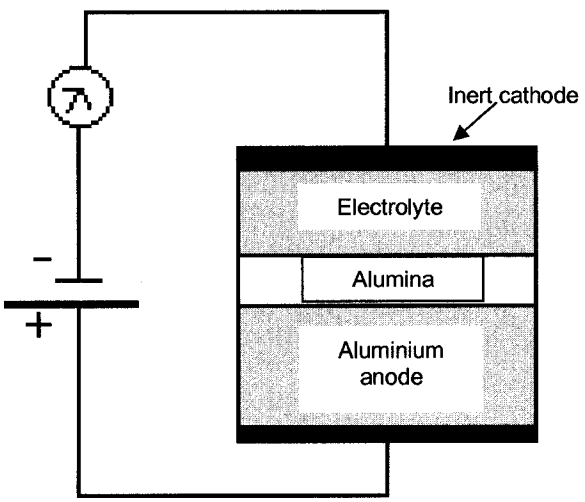

Figure 2.3: Simple schematic of anodizing setup

In normal conditions, a thin alumina barrier layer covers aluminium surfaces. This thin barrier layer reaches only a few tens of nanometers in thickness and stops growing [9]. This layer protects the aluminium surface from further corrosion, and scratches, since it is a harder material. Anodizing, however, creates alumina in a different way than oxidation occurring under ambient conditions.

Just like in ambient temperature, the anodized alumina layer first starts forming as a barrier type layer. As it thickens, the pores develop, and the oxide grows as a porous membrane [9]. The barrier layer remains at the bottom of the porous membrane, and forms a "barrier" between the aluminium surface and the porous aluminium oxide. The interface between the porous array and the barrier layer forms a semi-spherical shape, as shown on figure 4.

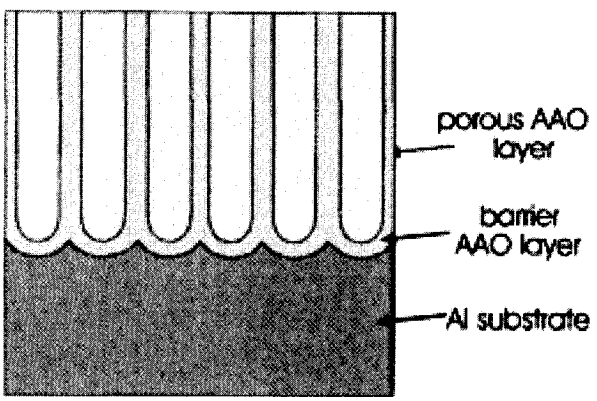

Figure 4: Shows the separation of the alumina and the porous alumina by the alumina barrier layer [10].

Figure 2.4: Shows the separation of the alumina and the porous alumina by the alumina barrier layer [10].

During anodizing, the aluminium piece serves as the anode by connecting it to the positive terminal of a DC power supply. The cathode, a plate of any electronic conductor that

is inert in the anodizing bath (ex: carbon, lead, nickel or stainless steel) is connected to the negative terminal. Once the circuit is closed, electrons are withdrawn from the metal at the positive terminal and allow ions at the metal surface to react with water to form the oxide layer on the surface of the metal. The electrons return to the bath at the cathode where they react with hydrogen ions to make hydrogen gas [10].

2.2.3 Electrochemical reaction during anodizing

Metals that can be anodized oxidize quickly with oxygen in air, so, when under ambient conditions, the surface of the metal is always covered with a thin oxide film. The film structure and composition depend on the length of exposure to ambient atmosphere. Aluminium, however, develops a barrier oxide layer on top of the metal that is only a couple of nanometers in thickness. The barrier oxide layer stops further reactions due to its environment. This layer is also an excellent electrical insulator. When an aluminium piece covered with this oxide is connected as an anode inside an electrolytic cell, current flows is significantly inhibited until the voltage is raised passed 1 or 2 volt. This oxide can support an electric field of up to 1 V/nm [17]. At this stage, oxygen evolution still does not occur, since the oxide acts as a barrier, stopping electrons from migrating from the electrolyte to the metal. The voltage across the oxide can therefore be increased without instigating current flow, until the field is large enough to drive aluminium and oxygen ions through the oxide. The oxide layer is formed by the reaction of the ions of this ionic current passing through the oxide. The O2- move inward to react with aluminium at the metal/oxide interface and forms the oxide at that point. The Al3+ ions move from the metal to react with water at the interface of the oxide and electrolyte to form aluminium oxide (Al2O3) at that surface. At the cathode, the circuit is completed by the reduction of hydrogen ions to hydrogen gas [12]. Figure 5 illustrates these phenomena. The current density determines the thickness of the oxide. The

field in the oxide does not change as the oxide thickens, and only depends lightly on the current density and temperature of the system. The voltage however increases proportionally to oxide thickness. And since this whole reaction is exothermic, the temperature of the system will increase. Thickness is very uniform throughout the surface since the voltage drop must be the same across the surface.

The overall reaction which occurs during the anodizing process takes place as follows [12]:

$2Al + 3H2O \rightarrow Al2O3 + 3H2$

The above reaction represents the sum of reactions that happen at the anode and cathode. These reactions are explained in more detail in section 2.2.3.1.

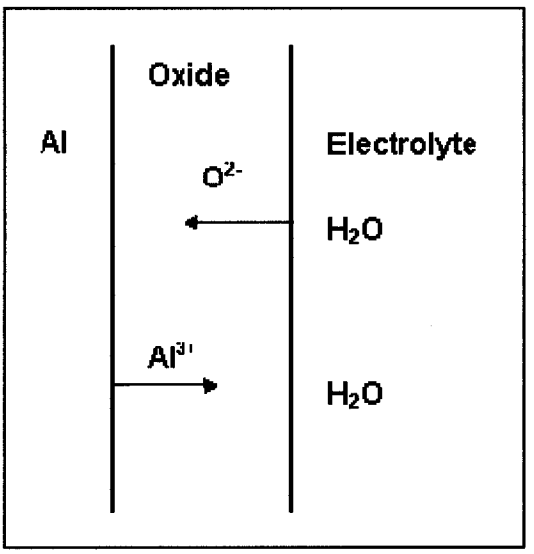

Figure 2.5: Illustrates how ions migrate during anodizing process [12]

2.2.3.1 Anodic reactions

The reactions at the anode occur at the metal-oxide and oxide/electrolyte interfaces. At the metal-oxide interface, the incoming oxygen anions react with the metal, causing the following reaction [12]:

$2Al + 3O2- \rightarrow Al2O3 + 6e-$

Outgoing aluminium cations react with water at the oxide-electrolyte, producing the following reaction [11]:

$2Al3+ + 3H2O \rightarrow Al2O3 + 6H+$

2.2.3.2 Cathodic reaction

Hydrogen gas evolution is the reaction that occurs at the cathode, and is described by the following equation [12]:

$6H+ + 6e- \rightarrow 3H2$

Anodizing baths usually have the ability to retain a high in- solution concentration of aluminium regardless of the electrolyte in use. This is essential, since a large portion of the aluminium that is oxidized passes into solution, and is not retained in the oxide film. For example, for anodizing experiment done in sulfuric acid, about 60% of the oxidized aluminium is in the film while the remainder is found in solution [15]. Due to its unique structure, it is easy to make porous films that are about 100 times thicker than the barrier film, since, unlike barrier films, a high voltage is not needed [15].

2.2.4 Porous Morphology of anodized alumina

The electrochemical anodizing reactions have been known and understood for quite some time. However, the physical mechanisms underlying this remarkable self-organization process are not yet understood. Nevertheless, some compelling but incomplete theories and models have been developed through research. For example, a mechanical stress mechanism has been suggested in order to explain the self-ordering of the pores in anodic alumina [23]. It was discussed that the neighbouring pores, having repulsive forces due to the mechanical stress at the metal-oxide interface, promote the formation of a hexagonally ordered pore arrangement. This theory brings rise to the belief that, the volume expansion supplementing

the aluminium oxidation induces the mechanical stress at the aluminium-oxide interface. This expansion depends greatly on the experimental conditions (choice of electrolyte and anodizing voltage).

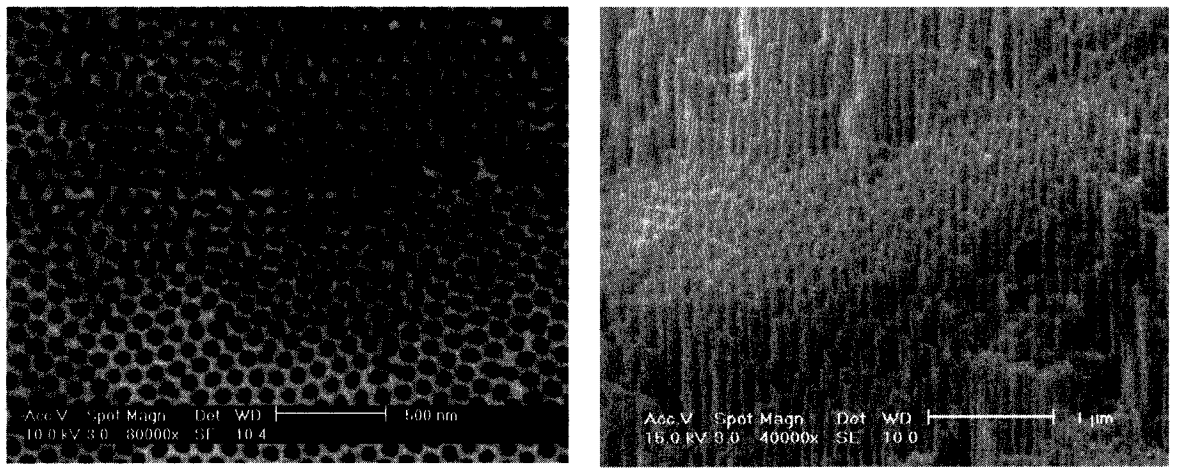

Figure 2.6: (a) Top view and (b) cross-sectional view of a highly ordered anodized aluminium oxide layer with pore diam. of approx. 55nm.

No matter how polished, a metal surface always has some degree of roughness. This may be due to the fabrication process, from chemical etching, or prepping the sample before anodizing it. Even electro-polishing, the most effective polishing technique creates a scalloped surface texture with shallow cells of the order 100 nm in diameter [16]. During early growth, the film above the elevated parts of the surface becomes thicker than in the depressions. It seems that ions move through oxide more easily at these locations. This may be because of higher film stress, impurities, or oxide flaws, simplifying current concentration at these locations. This happens temporarily, until the current shifts towards the thinner oxide in depressions, giving the oxide acquires more uniform properties. Since there is a concave geometry developed, the electric field is slightly higher inside the depressions, and field-assisted dissolution promotes local oxide thinning and current concentration. Small pores

are deepened further, as the electric field and the dissolution rate between pores decrease. The morphology adjusts until a steady state governs the rest of the film growth, and deep pores continuously grow as the anodizing continues at a speed of about 1-2 μm/h.

Masuda and Fukuda [24] reported large regions free of defect developing in large domains, while at the boundaries of these domains, defects were found after a long anodization period. The long anodization time rearranges the cells and reduces the number of defects and dislocations. It was also showed that pores tend to nucleate in regions of increased surface elastic energy and grain boundaries are typically preferred sites [13]. There is no direct evidence, as of yet, that defects in the pore lattice can originate from dislocations or other defects in the aluminium. However, it is clear that the self-organization is disturbed by a large number of grain boundaries in the non-annealed aluminium foils. Barrier oxide and pores at depressions form faster on high surface roughness areas compared to other smoother locations. The pores that were formed at such dips will grow earlier than at other sites. The surface roughness can therefore prevent self-organization. However, stirring the electrolyte could contribute to a more homogenous etching condition. Prepping the sample by annealing the aluminium sample can increase the grain size and have a more homogeneous cubic texture, while stirring of the electrolyte during oxidation, and using smooth electro-polished aluminium surfaces are all necessary for obtaining ordered hexagonal structures with typical long-range ordering of 100 μm^2 [11].

The formation of pores upon anodizing varies depending on the oxidation rate of the sample, the field enhanced oxide dissolution rate at the oxide-electrolyte interface. These in turn depend on the applied voltage, and the type of acid electrolyte used. These factors can be controlled in order to properly create homogeneous pores [9, 19]. It has been found that the inter-pore distance can be controlled by controlling the voltage. The inter-pore distance can be adjusted from 50-420 nm depending on the applied potential [20]. At low potentials

ranging from 30 to 60 volts (depending on the acid) can lead to inter-pore distances of 50-150 nm. Higher potentials, ranging from 100-160 volts, yield inter-pores distances raging from 300-420 nm [20]. It can also be established as a rule of thumb that the pore diameter is estimated at 30% of the inter-pore distance.

It has been proven recently that the shape of the cross-sectional opening can be altered by pre-texturing the surface of the aluminium. In 2004, Yanagishita et al. showed that they where able to create an anodic alumina template by the nano-indentation of aluminium using a mold with a convex array of graphite lattice arrangement. The concave pits acted as initiation sites of the pores and an anodic porous alumina membrane with triangular opening was produced [22].

2.2.5 Two step anodizing process

It has been shown through literature that a two-step anodization process can improve the pore regularity. In this process, the substrate is re-anodized after stripping away the thick aluminium oxide film obtained from the first long anodization. A porous thin alumina film with highly ordered pores can be obtained by this second anodization [11, 25, 26]. Figure 7 displays this two step anodizing procedure.

The first anodizing process serves as a pretexturing step for the aluminium substrate. Once relatively disordered oxide layer formed during the first anodizing step is removed through an etching process in sodium hydroxide, it leaves a uniform concave nano-array. This array is crucial in order to obtain a much more uniform and ordered array during the second anodizing procedure produces.

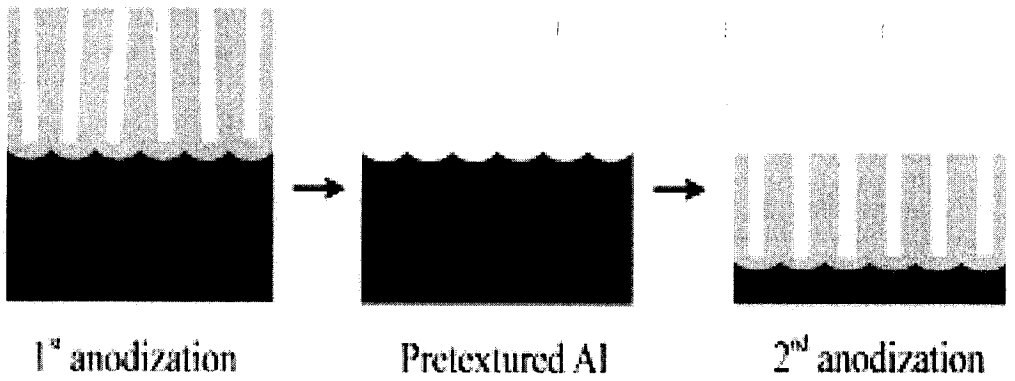

Figure 7:

Figure 2.7: Two step anodizing [10]

After the second-step anodization, the porous alumina is still standing on top of the aluminium substrate. It is possible to separate the porous oxide layer from the Al base by an etching process. Further processing into a freestanding membrane of nanopores that is open on the top and bottom is possible [10]. This free standing porous layer can be used as a base template stencil or mask for fabricating a variety of highly ordered nanostructures. There are many advantages of this non-lithographic fabrication method using very organized, highly ordered anodized aluminium oxide nanopore template. These advantages include:

→ controllable 20 to 200 nm uniform pore diameter;

→ uniform inter-pore distance ranging from 50 to 400 nm;

→ highest packing density 109–1011 cm−2 due to the hexagonal symmetry;

→ Anodized Aluminium Oxide template pattern completely replicable onto the surface of a receiving substrate;

→ ability to make large areas;

→ low cost (especially when compared to e-beam lithography)

→process is not material specific ranging from oxides to semiconductors to metals to polymers;

→ compatible with existing IC processing, but not limited to existing wafer sizes;

→ process conformal to uneven surfaces either flat or curved, locally and throughout.

2.2.6 Producing nanostructures through electrodeposition on the anodized alumina template

From these templates, it is possible to "grow" nanostructures inside the nano-metric pores by electrodepositing materials inside them. The two most common ways of depositing materials inside these templates is through electrodeposition (also called electroplating), and chemical vapor deposition. These are the two methods that are commonly found in the literature as a means of depositing metals inside the pores of the anodized alumina.

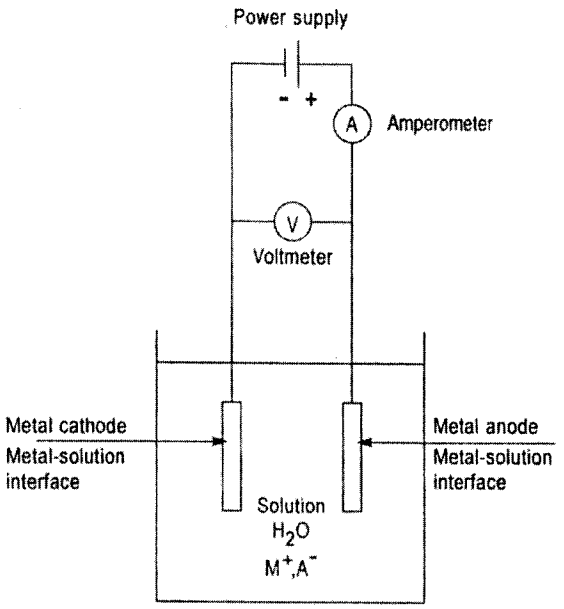

Figure 2.8: Electrodeposition cell setup for depositing the metal M+ from the solution containing the metal salt MA [27]

2.2.6.1 Electrodeposition:

Electrodeposition is the process of producing a coating, commonly metallic, on a surface by the means of an electric current. The deposition of a metallic coating onto an

object is achieved by putting a negative charge on the object to be coated and it is then immersing it into a solution containing a salt of the metal desired for deposition. Hence, the object to be plated is made the cathode of an electrolytic cell. The metallic ions of the salt carry a positive charge and are attracted to the substrate. When they reach the negatively charged object, it provides electrons to reduce the positively charged ions to metallic form. Figure 8 shoes the setup of an electrodeposition cell, where "M" is the plating metal from a solution containing the metal salt "MA".

By placing the free-standing template on a desired substrate (ex: silicon wafer), it is possible to electrodeposit almost any metal inside the pores, and produce nanostructures. Once the nanostructures are produced, revealing them is done by a simple oxide removal step [39,40].

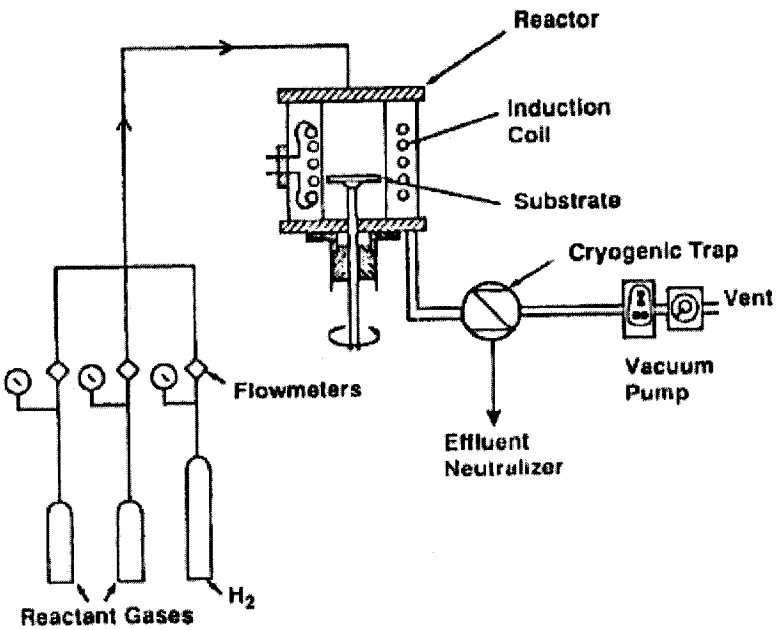

Figure 2.9: Typical CVD apparatus [28]

2.2.6.2 Chemical Vapor Deposition (CVD):

Although there are many different methods of CVD (ex: atmospheric pressure CVD, low pressure CVD, laser CVD, etc...), all or most rely on pretty much the same physical process. CVD is a chemical process used for depositing thin films or ultra fine powders of various materials. In a CVD process the substrate is exposed to one or more volatile precursors, which react and decompose on the substrate surface to produce the deposit. Usually, volatile by-products are also produced. These by-products are eliminated by gas flow through the reaction chamber.

CVD is a process widely used in the semiconductor device fabrication process, to deposit various films including: polycrystalline and amorphous silicon, silicon oxide, silicon germanium, tungsten, silicon nitride, silicon oxynitride, titanium nitride, and various other dielectrics [26].

As mentioned before, both techniques can be used in order to create different types of nanostructures. Depending on the processing manner, the desired nanostructure is achieved. The various types of nanostructures that can be processed are shown in figure 10 below. Although the nanostructures will not be discussed thoroughly, a brief discussion on possible fabrication process and applications will follow.

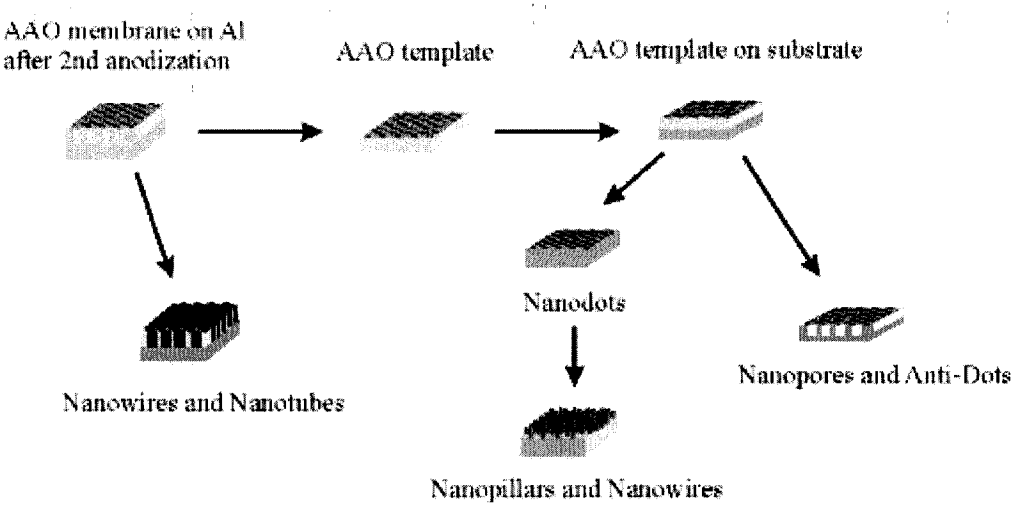

Figure 2.10: Diagram showing the different types of possible nanostructure arrays [10].

2.2.7 Nanowires and nanopillars

The primary advantage of using the porous alumina template is the ease of material handling. The aluminium substrate can be left as both a mechanical support and electronic contact during deposition. Since the thickness of the oxide layer can be varied, the length of wires or pillars can also be controlled. Various metals such as Ag, Fe, Ni, and Bi have been deposited into the pores of anodic alumina by an alternating current deposition technique [40,41,42]. Some have even gone further as to study the magnetic properties of Ni nanowires [43]. Alternating current is found to be effective due to the restrictions caused by the barrier layer of the anodized template, and also accommodates diffusion in the nanopores.

Electrodeposition processes have exhibited some drawbacks, such as the "sky-scraper" phenomenon. This refers to the lack of uniformity in length. This is due to the use of aqueous solutions. In these processes, the taller wires grow faster and taller than the shorter ones. Other drawbacks related to electrodeposition in aqueous solution are the need for a

conducting substrate, and the limited amount that can be deposited from aqueous electrolytes. Also, the quality of the nanowire arrays may be affected by oxidation of the metal. Ultimately, wire growth blockage can occur due to the sealing of the template pores. Fortunately, by replacing the electrolyte solution of the deposition process into a dimethylsulphoxide solution composed of metal chloride, the disadvantages stated above relating to aqueous electrolyte can be surmounted [29].

Some applications of metallic nanowires include X, gamma radiation and magnetic field sensing, as well as fundamental studies of nano-magnetics. The main interest here would be to consider the application of magnetic nanowires in areas such as electronics and nanodevices, metallic interconnects of nano devices, and especially in the field of magnetic storage.

2.2.8 Nanodots

Currently, through e-beam lithography, it is possible to write hundreds or even thousands of nanodot patterns in e-beam photo-resist with great accuracy and without extraneous efforts. But, when asked to write hundreds of millions of nanodots, the process would take an incredible amount of time and would also be limited by the microscopes field used to avoid stitching errors [11]. With the anodized alumina template, billions of closely packed nanodots of uniform size and spacing can be formed at the same time Through a series of simple processing steps.

Processing nanodots starts with removing the barrier layer and aluminium support, and leaving the porous alumina as a through-pore template. The template is then placed onto the desired substrate. This is usually done in solution since the membrane is very fragile and can be easily fractured in manual handling. Because of the Van der Waals force of attraction, the template bonds well to a flat substrate. Afterwards, metal layer can be evaporated through the

pores at a relatively slow deposition rate, since faster rates tend to clog the nanopores more easily. After peeling off or etching away the porous template, undesired metal is also lifted off, much like a conventional lift-off process in electron beam lithography. A perfect hexagonal array of metal nanodots is formed naturally on the surface of the substrate. Figure 2.11 is an example such a process. In that figure, a GaAs nanodot array was grown on a GaAs substrate. The mean diameter and spacing of the nanodots are limited by the pore diameter and spacing of the porous alumina membrane. Hence, by varying the inter-pore distance and diameter of the porous alumina, the diameter and spacing of the nanodots can also be controlled.

Possible applications for such technology include the development of nano-magnets for use in recording media and random access memory devices. Potential advantages of using such methods could include low-power dissipation, low interconnection demand, thermal stability at room temperature, and higher levels of integration and scalability [11].

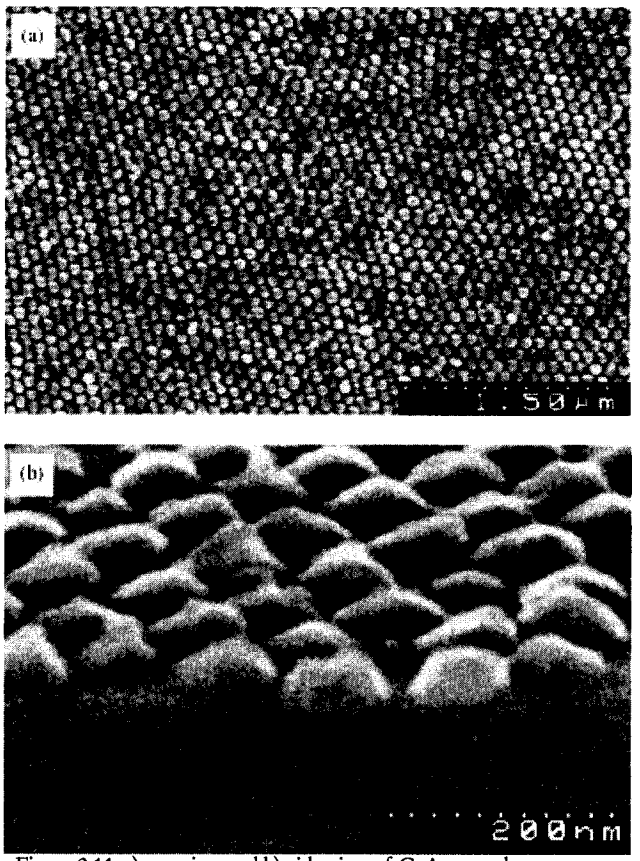

Figure 2.11: a) top view and b) side view of GaAs nanodots grown on GaAs substrate with the use of the porous alumina. [11]

The fabrication of nanopores is relatively simple. Once the anodized alumina template has been formed and the barrier layer removed, the nanopore array pattern is replicated through chemical or physical etching, in the substrate resulting in lateral superlattices of pores (commonly called anti-dots). Again, here, the size and spacing of the anti-dots can be controlled by manipulating the alumina template during anodizing.

One very interesting area where this technology can be employed is in the biomedical field. Scientists believe nanopores will allow DNA to pass through one strand at a time, and make DNA sequencing more efficient. As DNA passes through a nanopore, its shape and electrical properties of each base on the strand can be monitored. Because these properties are unique for each of the four bases that make up the genetic code (ATCG), scientists can

use the passage of DNA through a nanopore to decipher encoded information such as errors in the code known to be associated with cancer [30].

2.3 CONCLUSION

It is construable that the anodized alumina membrane as a template for nanostructure fabrication and its immediate contributions to nanotechnology is an up and coming field of research. The porous alumina membrane can determine the uniformity, the morphology and ultimately the properties of the nanostructures. By altering the anodizing conditions, the diameter of the pores and interpore distance in the alumina can be varied, depending on the anodizing conditions. Another alluring trait is the high packing density, covering an area that is rapidly scalable. Once this template is achieved, its use for nanostructure processing is not material specific, leading to an equal ease of use regardless of whether metals or semiconductors are used. This method also offers different shapes and sizes from a ranging amount of structures such as dots, tubes, wires, anti-dots, which can be fabricated with practically the same method. The versatility coupled with its ease of use and practicalities harmonize to the idea that this new and up-coming technology is very promising for nanotechnology.

CHAPTER 3: EXPERIMENTAL PROCEDURES

This chapter will discuss the synthesis of the alumina template. The first part of the chapter will include a short introduction on texture measurement and analysis. The rest is composed of 3 sections discussing substrate preparation (degreasing in acetone, heat treatment for cubic texture, x-ray diffraction, electro-polishing for a flat surface and low surface tension), anodizing conditions (electrolyte type and concentration, anodizing temperature, type of cathode, anodizing time) and template investigation through SEM, AFM, EDS, and powdered XRD.

The first part of the experiment represented results of a one step anodizing process. The second part of the experiment consisted of a second step anodizing procedure in order to study if the oxide was in fact more uniform. The first anodizing session was performed only for about 1 hour, since this step is used only to pre-texture the aluminium.

The second session was conducted for period of up to 3 hours. Before anodizing, the specimen was placed in a solution of 20% NaOH in order to strip the oxide layer from the surface of the aluminium.

3.1 SAMPLE CHARACTERISATION EQUIPMENT AND PROCEDURE

Samples were characterised with various instruments at different stages throughout the experiments. These instruments included a Secondary Electron Microscope (SEM) and Atomic Force Microscope (AFM), which were used to examine the morphology of the anodized alumina morphology, and an x-ray diffractometer in order to qualify the aluminium substrate and the created oxide film. X-Ray diffraction was performed with a Siemens D-5000 Diffractometer. The SEM used was a Philips XL-30 with Field Emission Gun.

3.2 TEXTURE MEASUREMENT PROCEDURES

Texture is the field in materials science which refers to the phenomenon of preferred crystallographic orientation of grains inside a polycrystalline material. Since many material properties are texture-dependant, this field of study is of technological importance. For some time, the only way to measure texture was though the means of X-rays on a rather large scale area. This provided average data for the entire sampled volume comprising thousands of grains on average. This method of texture determination is termed "macrotexture". In X-ray diffraction analysis, the texture is determined from pole figures. These pole figures are measured by recording the intensity distribution of a single set of Miller indices (hkl) reflection, by tilting and rotating the sample over the orientation sphere. In this way the orientation distribution for a single lattice plane is determined. When a set of pole figures for independent crystal orientations has been measured, the orientation distribution function (ODF) can be calculated. Later, with the development of Electron Backscattered Diffraction (EBSD), the examination of "microtexture" was possible. Microtexture can be defined as a population of crystallographic orientations in which individual components are linked to their location within the microstructure [32].

Many material properties have shown to be texture dependant. Some only depend on the orientation of crystallographic planes, and others on direction as well. A property that has shown dependency on orientation and direction is wear, while corrosion has shown dependency only on plane orientation. The effects of texture on certain aspects of anodized alumina topography will be investigated. There will be more focus given to macrostructure study, since this technique was used in the investigation relating to anodizing. A brief introduction on anodized alumina will be given later in this paper, but first an overview of texture will be covered.

3.2.1 Texture principles

For many, texture represents the structure of materials such as textile, wood, fibres, etc... For materials researchers and scientists, texture is a means of characterizing the orientation of grains in a polycrystalline material. It can be observed in almost all natural occurring and man-made materials. Texturing a material can occur through processes such as rolling, annealing, sintering and electroplating. It is important to study texture since it allows us to better understand various aspects such as metal transformation and variations in material properties.

In order to understand texture, it is important to first understand the principles in orientation of grains, and the two reference frames: the Crystal reference frame (Kc), and the Sample reference frame (Ks). As the name states, Kc is the reference frame with respect to the actual crystal inside the sample, while the Ks is the reference frame regarding the whole sample itself. The 3 axes in the Ks are usually represented with rolling direction, transverse direction and normal direction. It is possible to relate both reference frames through the Euler angles PHI (Φ), phi1 ($\varphi 1$) and phi2 ($\varphi 2$), inside the Euler space. The latter is a Cartesian 3-D space where the angles are represented. Euler angles are descriptions of

orientation involving sequential rotations of the crystal coordinate system through three angles with respect to the sample (or specimen) reference frame. It is then possible to represent planes and directions of planes inside a crystal through Miller indices (hkl) [33].

Figure 3.1 shows the rotations necessary to superimpose the sample coordinate axis system (shown in blue) onto the crystal system (red). It can be noted that note that the orientation can also be defined by an equivalent set of Euler angles which superimpose the crystal coordinate system on the sample coordinate system.

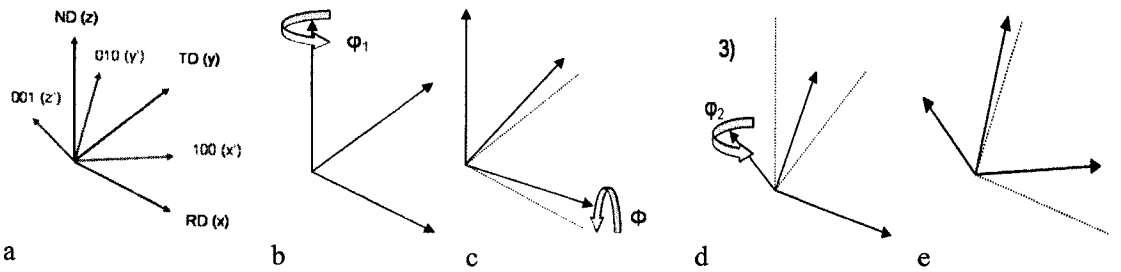

Figure 3.1: Example of how to relate Ks and Kc in Euler space [33].

In the example shown in figure 3.1, in order to relate both coordinate systems (a), the first rotation phi1 is about the z axis of the sample coordinate system (b). The second rotation is PHI about the new x-axis. The dotted lines show the positions of the axis before the previous rotation (c). The third rotation is phi2 about the new z-axis (d) and the final orientation (e) of the sample axis system is shown.

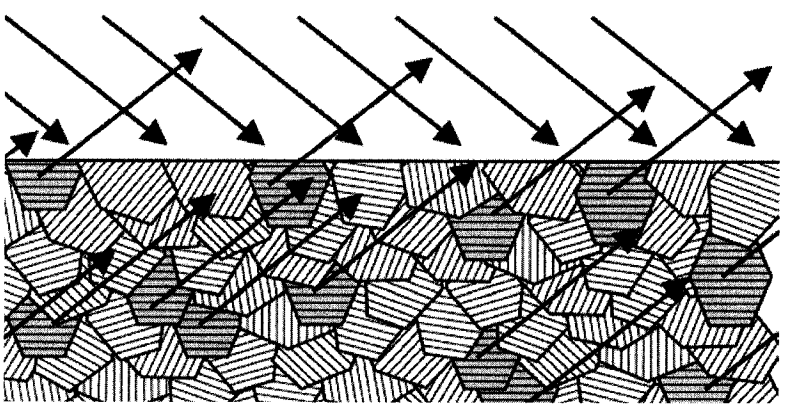

Figure 3.2: Crystallographic plane that satisfy the Bragg equation will diffract reflect x-rays [4].

In order to measure macrotexture, it is primordial to first find the angles at which the maximum intensities of x-rays are reflected. This can be found through a theta/2theta relationship and Bragg's law ($\lambda=2d*\sin\theta$). The sample is scanned by the diffractometer at every possible angle 2θ and X-ray intensity peaks which are characteristic to each material can be retrieved. These peaks in the x-ray diffraction pattern are directly related to the atomic distances (or lattice spacing). Hence, for a given set of lattice planes with an inter-plane distance of d, the condition for a diffraction to occur can be simply explained though Bragg's law, where λ is the wavelength of the x-ray and θ is the scattering angle.

Once the theta angles are known, it is possible to get different sets of pole figures for each of those angles. A pole figure is an angular distribution of a chosen crystal direction with respect to the specimen coordinate system.

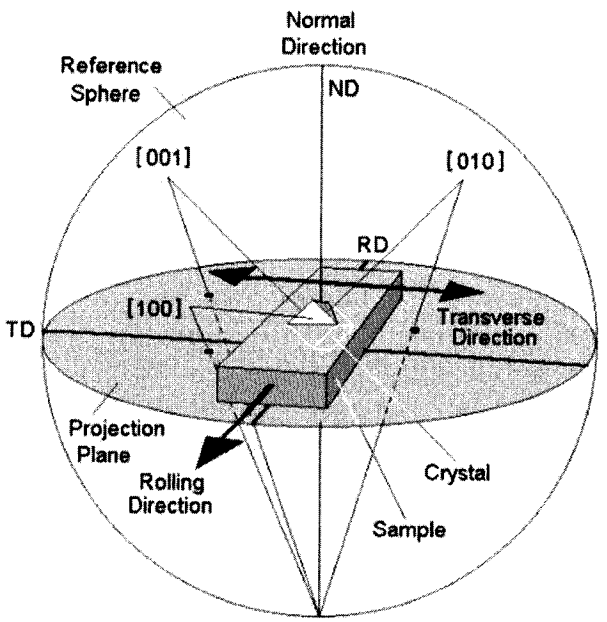

Figure 3.3: Stereographic projection displaying pole figure for {100} planes [33]

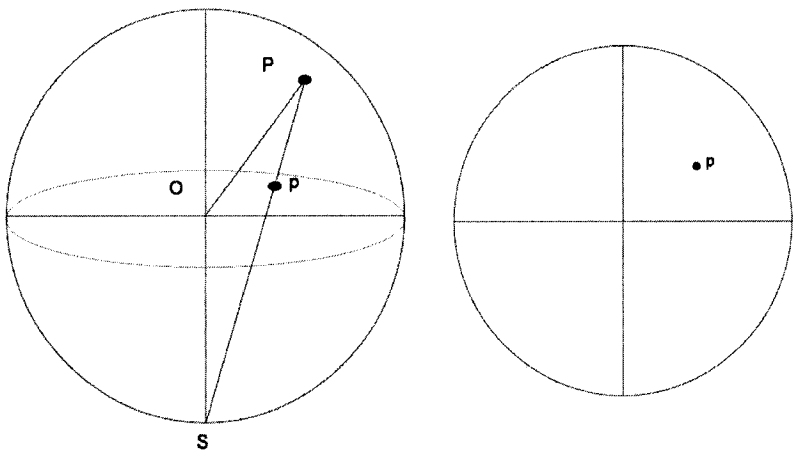

Figure 3.4: Projection of a point P on the surface of a sphere with centre O from the projection point S onto the equatorial plane at p [33].

The intensity of different poles is measured at a fixed scattering angle. This is repeated at the different scattering angles, yielding different pole figures.

Representing pole figures is done by stereographic projection, as shown in figure 3.4. This is a means of representing the pole intensities in a 2-dimentional figure. The manner in which this is done is shown in figures 3.3 and 3.5. In figure 3.5, the {100} poles are identified and extended to the surface of the reference sphere. From that point, a line is drawn to the south pole of the sphere, passing through the projection plane. The pole figure is actually the projection plane, and the points at which the lines cross the projection planes represent the poles. A larger population of points indicates a more intense pole, meaning that the orientation of that pole is predominantly present in the sample. Nevertheless, it is important to state that in order to have an accurate representation of the pole distribution; the sample must contain a relatively large amount of grains.

A better, more beneficial way of representing pole distribution is through inverse pole figures (IPF), which can be obtained from pole figures. Figure 3 shows the steps in

constructing the IPF from pole figures. Figure 3(b) shows the symmetry inside the projection plane. Since all the triangles formed represent the same area, only one triangle (shown in yellow in the figure) is necessary for IPFs. Figure 3.5(a) shows the creation of the IPF from the stereographic projection, where [110] and [111] poles are shown [33].

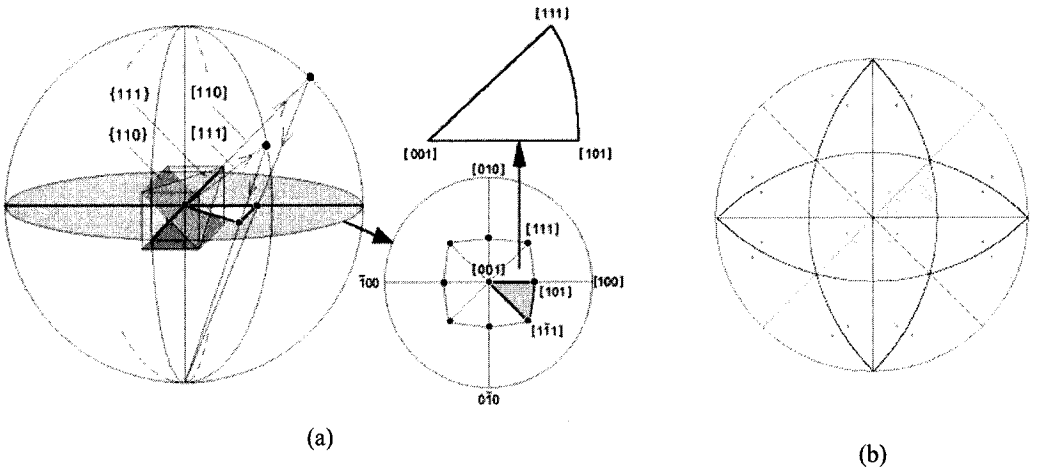

(a) (b)

Figure 3.5: (a) and (b): Summary of the steps involved in forming an inverse pole figure [33].

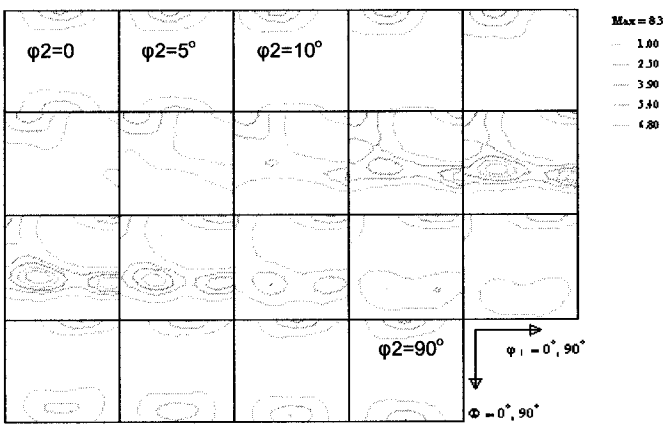

Figure 3.6: Example of ODF from stainless steel cathode substrate, calculated with TexTools ™ software.

The previous methods are useful when pole figures are concerned, but that alone is not enough to represent texture.. In order to characterize texture, it is mandatory to use the Orientation Distribution Function (ODF). This function is defined as the totality of all volume

elements (dV) of a sample (V) that has the orientation g within the element of orientation dg. This can be presented as: dV/V=f(g)dg. The orientation inside an ODFs is described in Euler angles, and is usually represented in 3-dimentional Euler space. From a set of pole figures, the ODF can be calculated, and is represented as shown in figure 3.6. Each point, inside each box of the ODF represents a certain orientation of the specimen. The first box represents angles φ1 from 0-90° on the top, Φ from 0 -90° on the side. The box at the top left corner represents φ2 equal to 0°, and increases in each box by 5 degrees. The second box is then equal to 5°, and so on, until the last box at the bottom right corner represents φ2 equal to 90°.

3.3 ANODIZING EQUIPMENT

A hydrogen permeation cell was modified to suit the anodizing process. The cell contained a 1 cm diameter opening were the aluminium was placed for anodizing. A rubber O-ring made the opening watertight to prevent the electrolyte from leaking during anodizing. Figure 3.5 is a cross-sectional drawing of the cell.

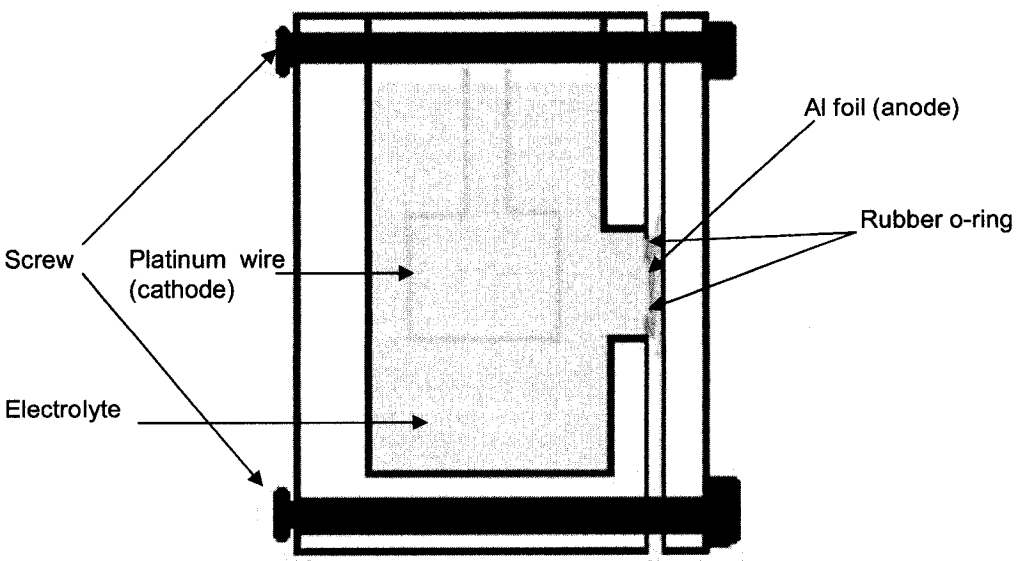

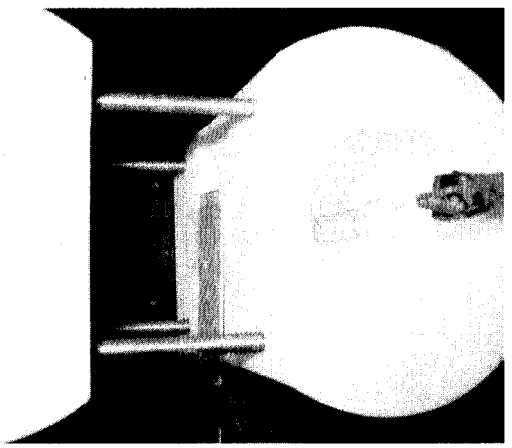

Figure 3.7: Anodizing cell

The type of acid used for anodizing was oxalic acid. Through literature, it was found that oxalic acid is frequently used for anodizing purposes. It is a weak acid, and therefore requires a higher anodizing voltage. Anodizing experiments where first done at 30 volts using a DC voltage source and were further increased up to 40 volts. A starting concentration of 0.3M was chosen for the electrolyte. These specifications were also taken from literature.

Lead and platinum anodes were used for anodizing during periods lasting up to 6 hours, with an electrolyte concentration of 0.3M. The anodizing time was increased until porous formation was visible through SEM investigation. The SEM used was a Philips XL-30 Field Emission Gun SEM. The concentration of the acid was increased to 0.6M for the series of anodizing experiments. Anodizing time was considerably reduced with the change in concentration, as can be seen in table 4.1. The same sequence of experiments was performed again after the increase in concentration. First a Pb anode was used for anodizing times of up to 6 hours, followed by anodizing experiments using a Pt anode for up to 6 hours as well.

Just like in ambient temperature, the anodized alumina layer first starts forming as a barrier type layer. As it thickens, the pores develop, and the oxide grows as a porous membrane. The barrier layer remains at the bottom of the porous membrane, and forms a "barrier" between the aluminium surface and the porous aluminium oxide. The interface

between the porous array and the barrier layer forms a semi-spherical shape, as shown on figure 2.4.

3.4 ANODIZING PROCEDURES

The aluminium substrate is placed inside the anodizing cell, insuring that it is fully covering the 1cm diameter opening. A longer aluminium plate is placed on the back to the foil in order to connect to the alligator clip leading to the negative terminal. This plate also serves as support for the foil during anodizing, since the foil is very fragile. The screws of the cell are tightened in order to prevent electrolyte leaks during anodizing, as well as to insure proper contact between the aluminium plate and the foil. The cell is then filled with the electrolyte, covering the exposed aluminium foil. The cathode is then immersed inside the cell, insuring that is remains directly in front of the 1cm diameter hole. The voltage meter is turned on to monitor the potential, and the voltage source is turned on, and adjusted to 40V.

Once the primary anodizing is complete, the anodized foil is carefully removed from the cell and immersed in alcohol for 10 seconds. The foil is then taken out of the foil and rinsed in distilled water. It is then placed inside a 20% NaOH bath for a maximum of 15 minutes in order to dissolve the oxide layer formed. The sample is then rinsed in distilled water and replaced inside the cell for the secondary anodising process. When placed in front of a light source, the completed anodized portion of the foil (1cm diameter circle) should be translucent, and it should be possible to fully discern shapes and colors when looking through the sample. A simple and swift examination of the sample is performed through the SEM to ensure that the sample was anodized through the foil. If not, the sample is carefully reinserted inside the cell and the anodizing process is restarted. If the sample was anodized through, it is then put through the pore widening process by immersing it in 5% H_3PO_4. The sample is then inspected again to insure that the pores are wide, and that the barrier layer has been removed.

If the pores of the back of the template are still not clearly visible, the pore widening step is repeated. Once these steps have been successfully achieved, the sample is ready to be used as a template for electrodeposition. The electrodeposition method is explained later in the report.

3.5 ELECTRODEPOSITION EQUIPMENT

Nickel nanowires synthesis was attempted through electrodeposition. A Watts bath, composed of nickel sulfate, nickel chloride and boric acid, was used due to its proven efficiency. Multiple template preparation steps where performed in order to promote deposition. Multiple electrodeposition experiments where performed until parameters permitting superior and reproducible results where obtained when observed through the SEM.

After the pore widening treatment, a layer of gold-palladium was deposited on the reverse side of the template. The deposition was done using a Hummer 6 Sputter Coater used to coat non-conductive samples for SEM analysis with a Au-Pd target. This coating process was complete after 15 minutes. The backside of the sample was then inspected with the SEM in order to insure that the sample was thoroughly covered, but the pores were not filled. If the coating was inconsistent, another coating process was performed.

Using the sputtered layer as a conductive layer, nickel nanowires were processed on the alumina template through electrodeposition. Using an AutoMet potentiostat as an electrodeposition source, the sample was placed in the same anodizing cell for the deposition process. A Watts bath was used as an electrodeposition solution due to its proven efficiency. Prior to being placed in the deposition cell the template was rinsed using nano-pure water. A platinum wire served as a cathode, and the template itself acted as the cathode. A SCE reference electrode was calibrated and used to monitor the deposition process.

An preliminary high current of 0.02 A was imposed during the deposition process for 5 seconds in order to induce deposition, and then lowered to 0.01 A for 50 seconds in order to

deposit nanowires inside the pores. The current was monitored with the GPES (General Purpose Electrochemical System) software.

CHAPTER 4: ANODIZING RESULTS

This chapter will report the results achieved from the anodizing experiments. First the anodizing method will be discussed, beginning with sample preparation and followed by anodizing procedures. The subsequent anodizing results are presented, showing the different effect of altering different variables such as acid concentration, voltage, cathode material and anodizing time.

4.1 SAMPLE PREPARATION

Before anodizing, it was necessary to prep the sample in order to get meaningful results. Substrate preparation consisted of annealing, degreasing and electropolishing the pure aluminium. The annealing was done at 430^0C for 5 hours. This is performed in order to acquire strong cubic texture. Pole figures from certain samples were generated, and will be discussed in chapter 5.

The aluminium surface was electropolished in a solution of 60% H3PO4 and 40% H2SO4 (volume fraction) at a DC voltage of 10V for 1 minute. This process which occurred at around 50^oC, removed around 1 um of aluminium from the substrate surface.

4.2 ANODIZING EXPERIMENT

One-step and two-step aluminium anodizing experiments were performed on a 99.998% 0.5 mm thick pure Aluminium plate in 0.3M oxalic acid, using a 40V potential. Experiments were run using two types of electrodes: lead and platinum. Anodizing was performed to lengths of up to 7 hours in the polymer anodizing cell shown in figure 3.1. As expected, the length of the anodizing period had a direct effect on the depth of the porous oxide film.

Once the sample was ready for anodizing, it was degreased in acetone for duration of 5 minutes, and anodized under the previously described conditions. After anodizing, the template was rinsed in distilled water, and immersed in a solution of 5% H_3PO_4 for 25 minutes. This was a pore widening process, in order to facilitate SEM investigation by lowering the charging effect. Charging creates a blur during analysis due to a charge build-up on the top of non-conducting materials.

4.3 ANODIZING RESULTS

Table 4.1 comprehensively shows the anodizing results with respect to the acid concentration, type of anode and time of anodizing. Some samples went through a second anodizing step of 3 hours, while the others only experienced a one-step anodizing step. Nevertheless, results were very similar if not identical.

The anodizing time was increased until porous formation was visible through SEM investigation. Figure 4.1A shows the 6 hours anodizing results using a lead anode in 0.3M oxalic acid. The experiment resulted in very shallow pores, with large areas of non-uniform aluminium oxide. Figure 4.1B is from a 6 hour anodizing experiment using a platinum electrode in 0.3M acid. Results such as shown in figure 4.2 were achieved after a period of 6 hours using the lead electrode, and 5 hours using the platinum electrode with an acid concentration of 0.3M. Figure 4.2 shows the 6 hours anodizing results using a lead anode in 0.3M acid. The experiment resulted in very shallow pores, with large areas of non-uniform aluminium oxide. Figure 4.3 is from a 6 hour anodizing experiment using a platinum electrode in 0.3M acid. Results in both cases were unsatisfactory. It was also difficult to generate a good SEM image because of the charging effect caused by large amounts of oxide on the sample surface. When the concentration was increased to 0.6M, substantial results were achieved after only 3 hours.

Table 4.1: Anodizing results

Acid Type	Acid Concentration	Anode	Anodizing time (hrs)	Results
Oxalic	0.3M	Pb	1	-
Oxalic	0.3M	Pb	2	-
Oxalic	0.3M	Pb	3	-
Oxalic	0.3M	Pb	4	-
Oxalic	0.3M	Pb	5	-
Oxalic	0.3M	Pb	6	poor
Oxalic	0.3M	Pt	1	-
Oxalic	0.3M	Pt	2	-
Oxalic	0.3M	Pt	3	-
Oxalic	0.3M	Pt	4	-
Oxalic	0.3M	Pt	5	-
Oxalic	0.3M	Pt	6	poor
Oxalic	0.6M	Pb	1	poor
Oxalic	0.6M	Pb	2	fair
Oxalic	0.6M	Pb	3	good
Oxalic	0.6M	Pb	4	good
Oxalic	0.6M	Pb	5	poor
Oxalic	0.6M	Pb	6	poor
Oxalic	0.6M	Pt	1	poor
Oxalic	0.6M	Pt	2	fair
Oxalic	0.6M	Pt	3	good
Oxalic	0.6M	Pt	4	v.good
Oxalic	0.6M	Pt	5	poor
Oxalic	0.6M	Pt	6	-

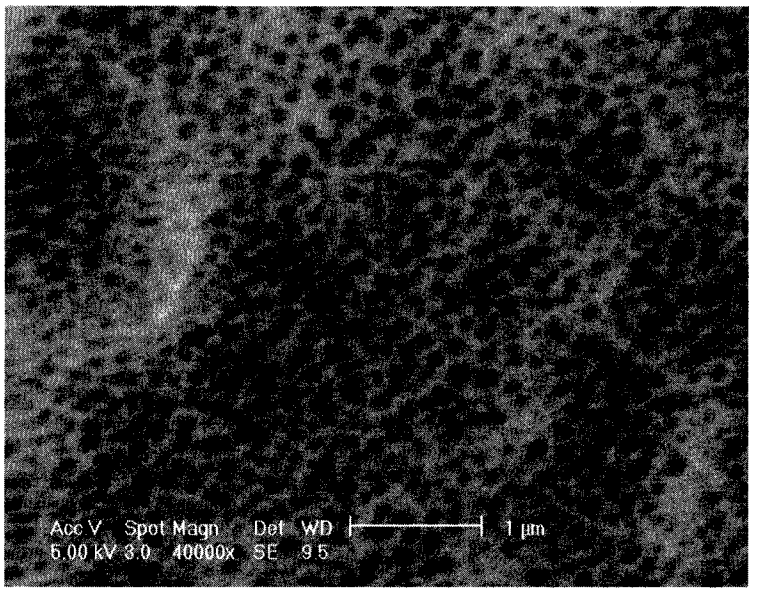

A

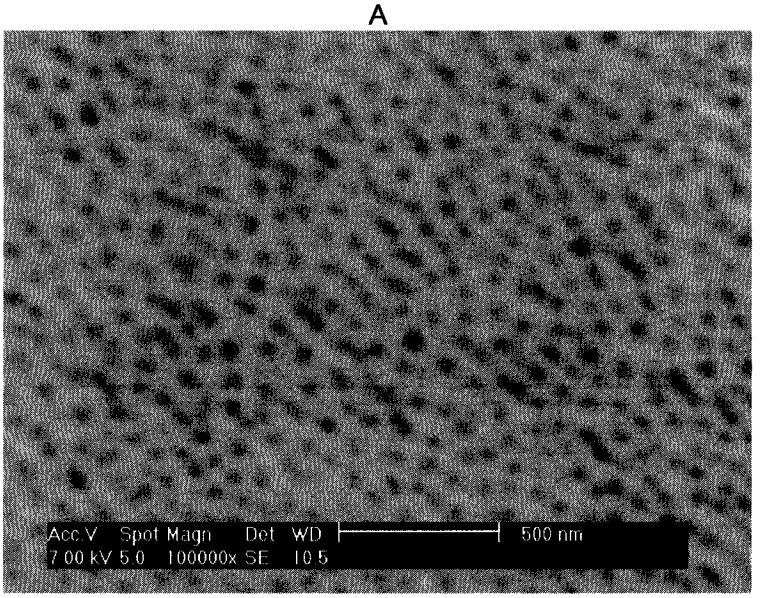

B

Figure 4.1: Pore structure and uniformity of anodized at 0.3M (A) and 0.6M (B) for 6 hours with Pt electrode

With an acid concentration of 0.6M, a significantly better outcome was achieved after a much shorter anodizing time of 3 hours. Figure 4.3 illustrates a more uniform, deeper pore structure obtained with a lead electrode, after 4 hours of anodizing. The following figure 4.4, is from the SEM investigation of a template acquired from 3 hours of anodizing, using a Pt anode. Both templates are very similar with regards to structure. The pore sizes and inter-pore

distances are comparable, but the results using the Pt anode are achieved with a shorter anodizing period.

The thickness of the anodized oxide layer can be seen on figure 4.7. The sample in this case was anodized using a Pt wire anode, in 0.3M oxalic acid for 2 hours. The oxide thickness was 20.8 um, which indicates an oxide growth of about 10 um per hour. Figure 4.6 is a cross-sectional image of the same sample, showing the long, columnar structure of the porous template. Again, the arrangement of the pores is regimented.

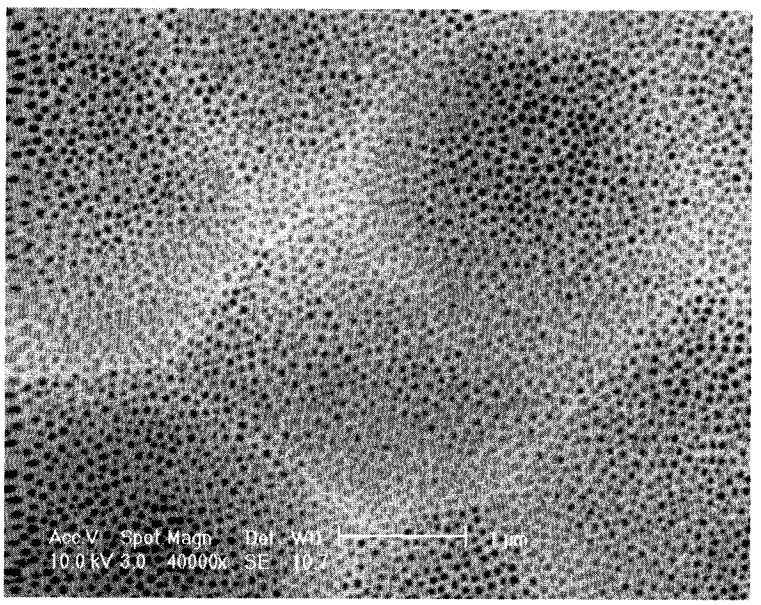

Figure 4.2 Pore structure and uniformity of sample anodized at 0.6M with Pb electrode

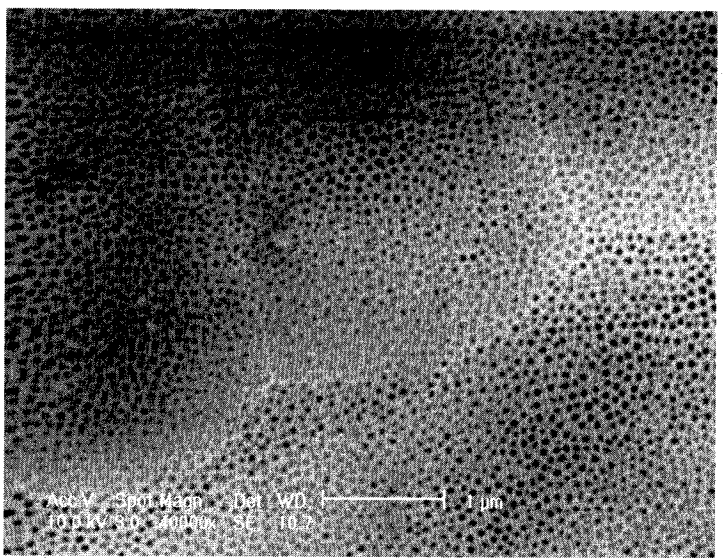

Figure 4.3: Pore structure and uniformity of sample anodized at 0.6M with Pt electrode

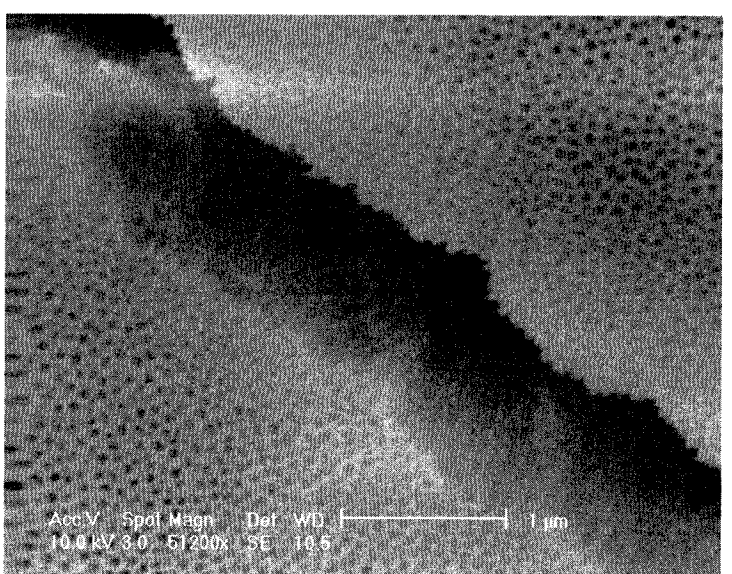

Figure 4.4: Pore structure and uniformity of sample that underwent 2-step anodizing process

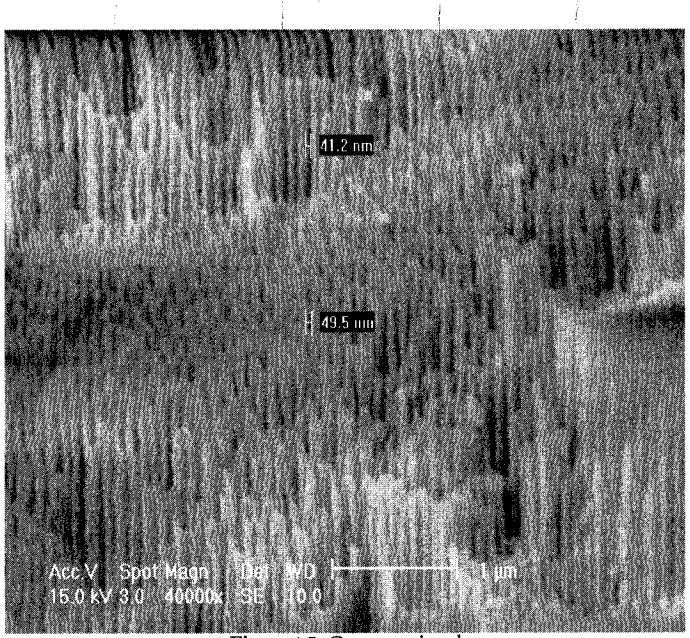

Figure 4.5: Cross-sectional morphology of an anodized sample

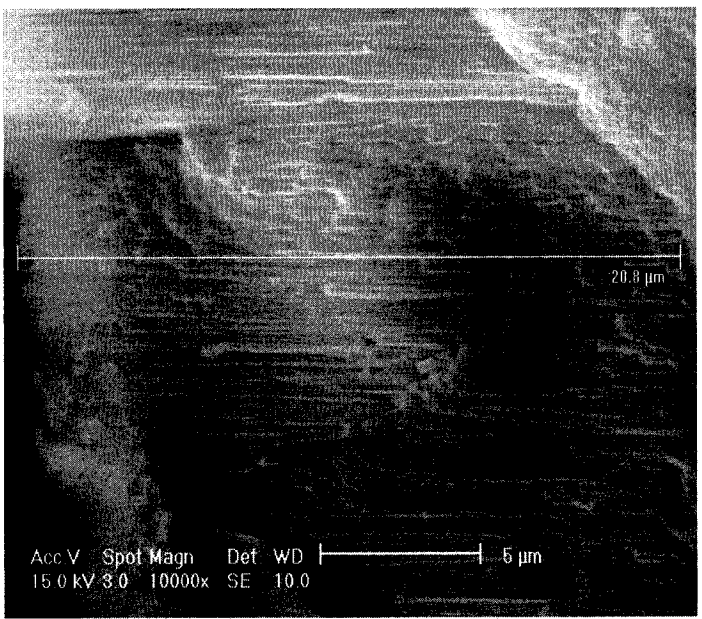

Figure 4.6: Thickness of anodized Alumina

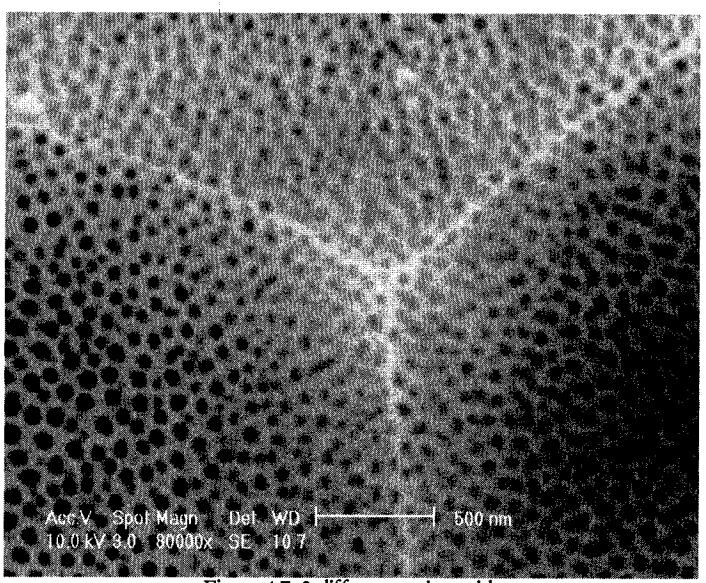

Figure 4.7: 3 different grains, with smaller pores close to grain boundaries

Once anodized, the pore widening step was performed. From figure 4.10, it is visible that the pores are much wider than when simply anodized. Figure 4.9A is a template that underwent a 2-step anodizing event, while figure 4.9B was subject to a 1-step anodizing event. Both images were taken before the pore widening step. As can be seen, both results are very similar, even though previous research has shown that a 2-step anodizing process yields significantly better templates.

An important discovery was made when looking at the back of the templates, when investigating if the barrier layer was completely removed during the pore widening process. The structure of the pores on the back were much more ordered and where much more uniform than the top of the template. Figures 4.11A and 4.11B show the highly structured pores of the back of the 1-step and 2-step anodized samples.

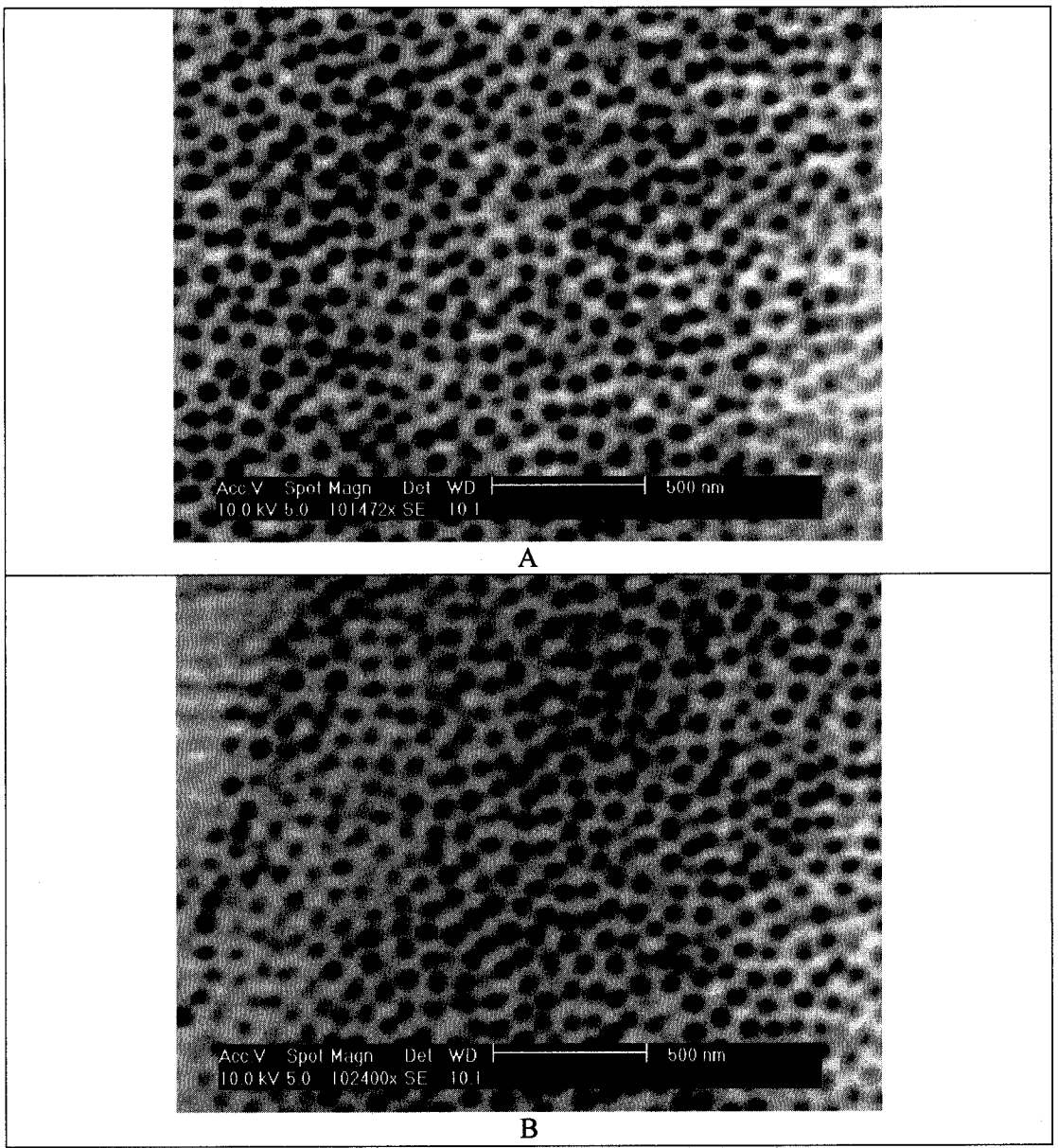

Figure 4.8: A) 2-step anodized sample, B) 1-step anodized sample

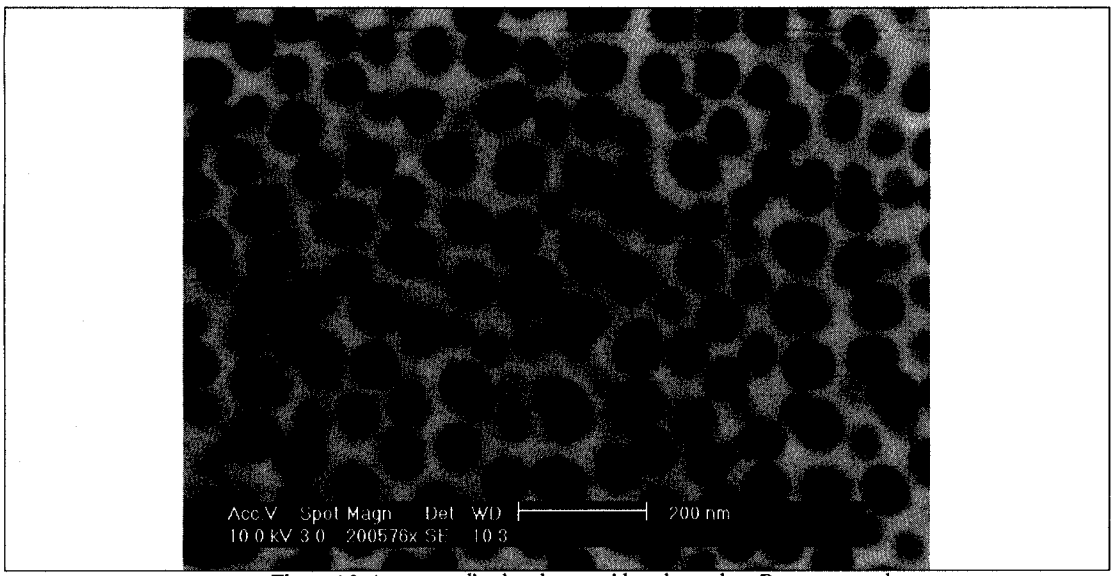

Figure 4.9: 1-step anodized and pore widened template. Pores are much bigger and more noticeable at higher magnification.

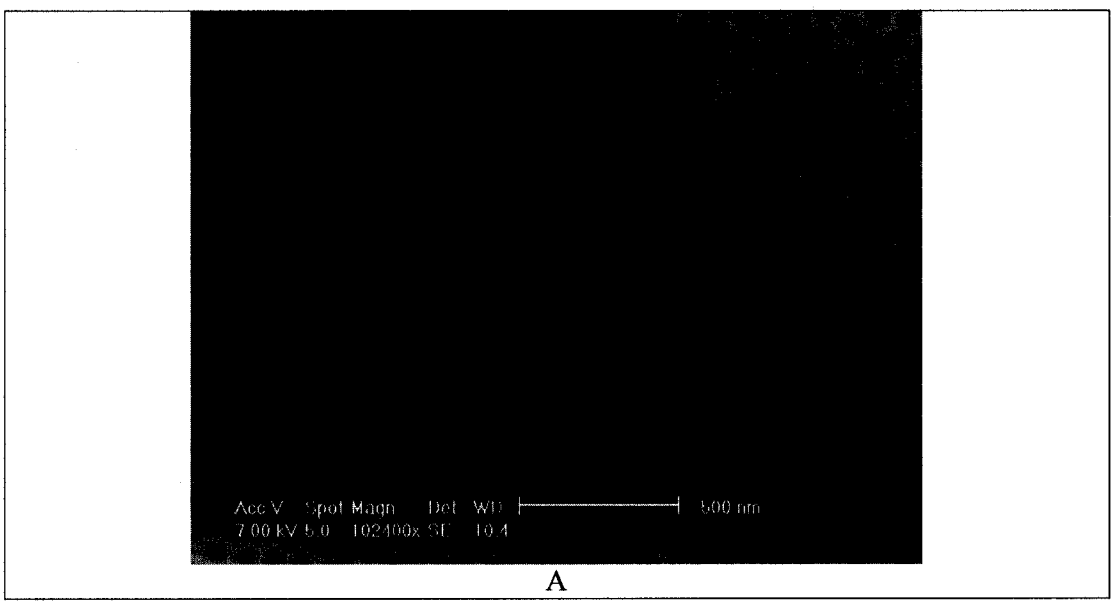

A

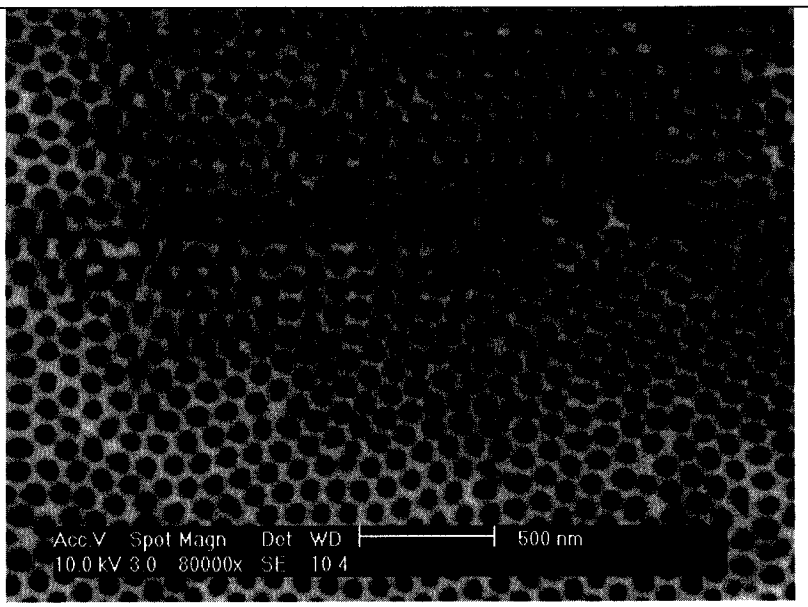

B

Figure 4.10: A) A: Back of 2-step anodized template, B) : Back of a 1-step anodized pore widened template. Hexagonal structure is very visible.

4.4 DISCUSSION

The samples anodized with 0.3M oxalic acid and a lead cathode yielded oxides were difficult to assess through the SEM. The oxides were thick, but pores were only very slightly discernable on the surface of the oxide. Increasing both the anodizing time as well as the electrolyte concentration did not seem to bring forth any improvements on the samples anodized with a lead cathode. Using a platinum wire cathode with an electrolyte concentration of 0.3M slightly improved the uniformity and depth of the pores, as was shown by comparing figures 4.1 and 4.2. Increasing the concentration to 0.6M reduced the anodizing time, but yielded only a slight improvement of pore uniformity and depth when a lead anode was used. The best results where obtained by combining the platinum electrode with a concentration of 0.6M oxalic acid.

After pore widening, the template was much easier to analyze under the SEM at a very high magnifications of 200576X, as seen in figure 4.5. The pores however seem less

structured then before the pore widening process, but the back of the template reveals very ordered and structured pores.

4.4.1 1-step and 2-step anodizing processes

After following the 2-step anodizing process, it was found that the changes in pore uniformity were not substantial enough to continue performing 2-step anodizing throughout the project. Surprisingly, the bottom side of the template was much more ordered than the top in both the 1-step and 2-step anodizing process. Therefore, subsequent templates where created using a one-step anodizing procedure, which created ordered pores but required less processing.

4.5 CONCLUSION

By altering the anodizing conditions, the diameter of the pores and interpore distance in the anodized alumina can be varied, depending on the anodizing conditions [38]. Ordered templates where created using both the 1-step and 2-step anodizing process. The final stage of research concerning the alumina template is to use it as a template for the processing and manipulation of nanostructures. To do so, a one-step anodizing process can be used to produce superior templates to be used for nanostructure processing. The following research objectives would be to first investigate the influence of aluminium purity on the template morphology, then explore the effects of grain size, grain boundary and texture on template morphology, and, finally successfully "grow" nanostructures inside the pores of the oxide layer though either an electrodeposition or electroless deposition procedure.

CHAPTER 5: TEXTURE EFFECT ON TEMPLATE MORPHOLOGY

This chapter pertains to the texture of the aluminium substrate and the effect it has on the formation of the pores of an anodized alumina template. Single crystal aluminium samples with different orientation were anodized in order to compare the resulting effects on the anodized alumina.

5.1 EXPERIMENTAL METHODOLOGY

By studying anodized alumina samples, it was found that the pore uniformity was not the same throughout an anodized sample. It was found that pore uniformity seemed to get distorted at grain boundaries, and some areas on certain grains were more uniform than on others. This can be noticed in on figure 4.7 of the previous chapter. The effect of texture on anodizing was therefore studied, in order to observe a possible relation between the orientation of the grain and the morphology of the template.

5.1.1 Sample preparation

A very large grain (approx. 10mm grains) sample was used in order to perform the study. Five different grains were cut from the sample in order to obtain small, single crystal aluminium samples. These samples were then mechanically polished from 800 grit paper to 1200 grit, and were electro-polished in a mixture of 80% perchloric and 20% acetic acid.

5.1.2 X-Ray Diffraction

X-ray diffraction was performed in a Rigaku diffractometer equipped with a rotating anode and a copper Kα radiation source. One of the samples was scanned in order to find the angles at which the diffracted x-ray intensities are the highest (2θ). Once those angles (2 in this case, 39° and 45°) were found, scans at both angles were performed on all samples inside the Seimens diffractometer. These angles are in accordance with results obtained by using Bragg's law, where the angles were found to be 38.47° and 44.74° for the first two intensity peaks. Other peaks could have been found simply by rotating the sample, but since the samples being used were single crystals, it was assumed that two pole figure generations were enough to give information on the orientation of the sample. This yielded the (111) pole

figure at a diffraction angle of approximately θ=190 and the (200) pole figures at a diffraction angle of approximately θ=22.50. An example of a pole figure generated for an anodized sample is shown in figure 5.2.

5.1.3 Orientation Distribution Function

[111] and [200] pole figures where obtained through x-ray diffraction. From these pole figures, ODFs were generated for each sample. The ODF was produced with the TexTools® software. The ODFs for each sample is shown in the results section.

5.1.4 Anodizing

Once the orientation of each sample was known, the next step was to anodize each sample. Each sample was anodized at a constant voltage of 40V, inside an anodizing cell containing 0.3M oxalic acid for a length of 4 hours, using a platinum cathode. Each sample was looked at in a Philips XL-30 FEG SEM. Pore size and uniformity was analysed, and the images showing these results figure in the results section.

5.2 RESULTS AND DISCUSSION

5.2.1 X-ray diffraction results (determination of 2θ)

The resulting x-ray intensity peaks shown below were obtained from the Rigaku diffractometer. The first peak represents the diffraction angle for the [111] plane, while the second represents the one for the [200] plane.

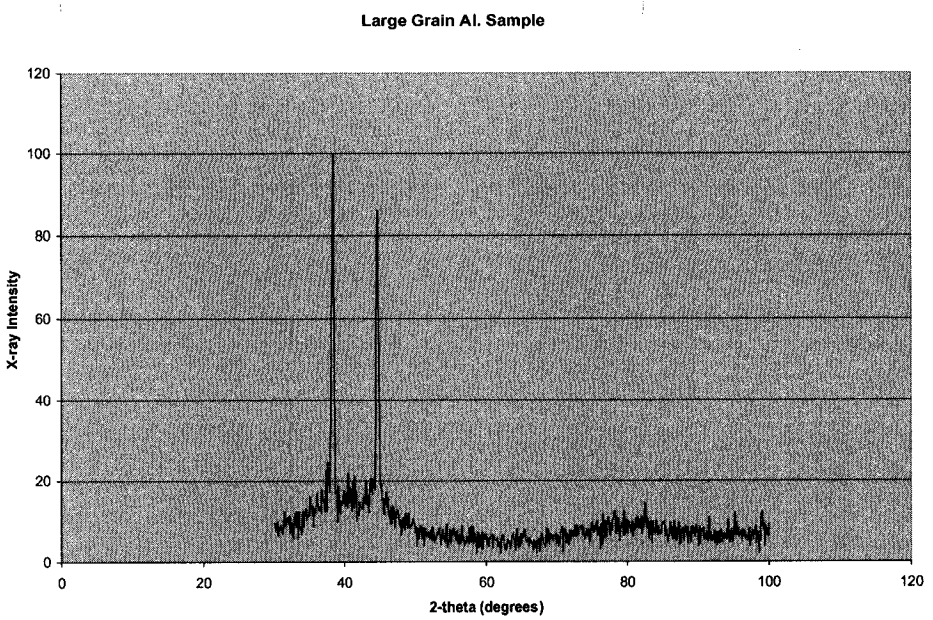

Figure 5.1 Characteristic x-ray peaks for aluminium

5.2.2 Pole figures:

The [111] and [200] pole figures where generated from data gathered from the Seimens diffractometer. The pole figures where calculated using the TexTool® software. Pole figures from sample 5 are shown in the results section, and table 5.1 displays the orientation of all 5 samples though their Miller indices (hkl), as well as their Euler angles. From the pole figures, it is noticeable that the [001] orientation is parallel to the surface of the specimen.

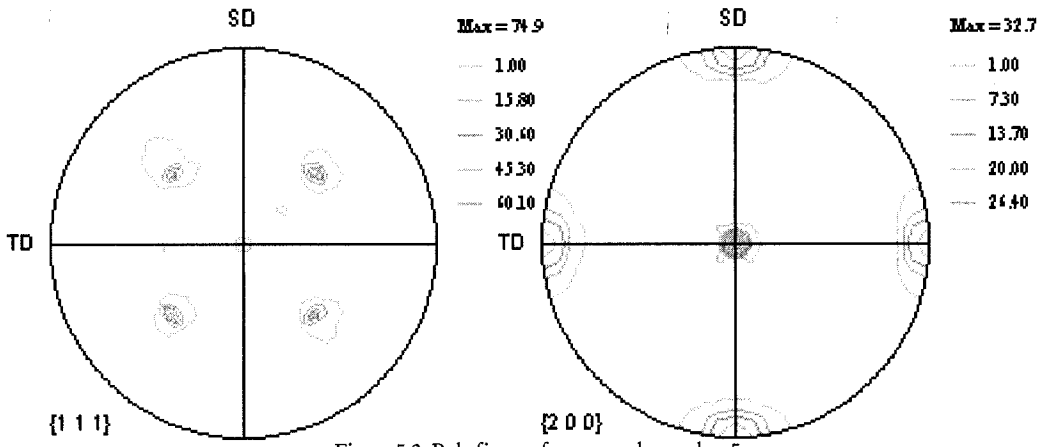

Figure 5.2: Pole figures from sample number 5.

Table 5.1: Orientation of each single grain sample

Sample	Euler angle	Miller Indices (hkl)
1	60, 35, 35	(235)
2	33, 29, 35	(113)
3	73, 35, 45	(324)
4	30, 1, 60	(001)
5	25, 1, 65	(001)

5.2.3 Orientation Distribution Function

From the pole figures obtained, an ODF was constructed for each sample. The ODF for sample 5 is shown below. The high maximum intensity (286.2) shows that the sample was indeed a single crystal. Nevertheless, being that the sample is a single crystal, texture is non-existent, since there is only one crystal present.

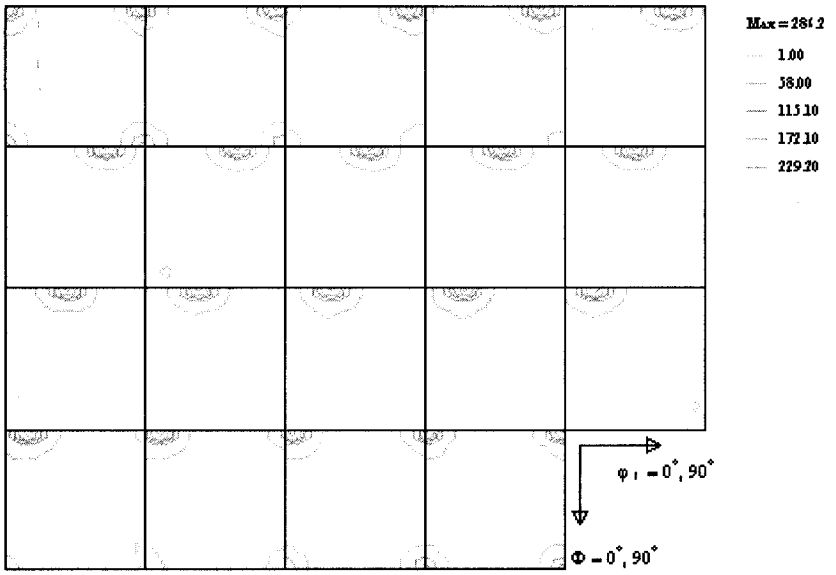

Figure 5.3: Orientation distribution function (ODF) taken from [111] and [100] pole figures. Is this ODF from the whole specimen, many grains?

5.2.4 Anodizing results:

After anodizing the samples were examined in the SEM in order to measure the pore size, and evaluate the uniformity of the pores formed though anodizing. Due to charging of the oxide layer, the image kept moving and it was very difficult to capture an accurate image that included the measuring bars. Nevertheless, images of samples 1 - 5 are shown. It is noticeable that there is not much of an order to the pores, which was the case for all the samples, except sample 3, which has a more distorted array. Also, the only relationship between the orientation and pore size is that both samples with (001) planes have very similar pore sizes. Table 2 below shows the relationship (or lack there of) between the plane orientation and the pore size of the anodized alumina. From this graph, the inverse pole figure was generated. It can be seen on the IPF that on both samples with (001) orientation, the pores sizes range from 55nm to 60nm. All the samples have similar pore sizes, except the sample with orientation (324), which has a larger pore diameter.

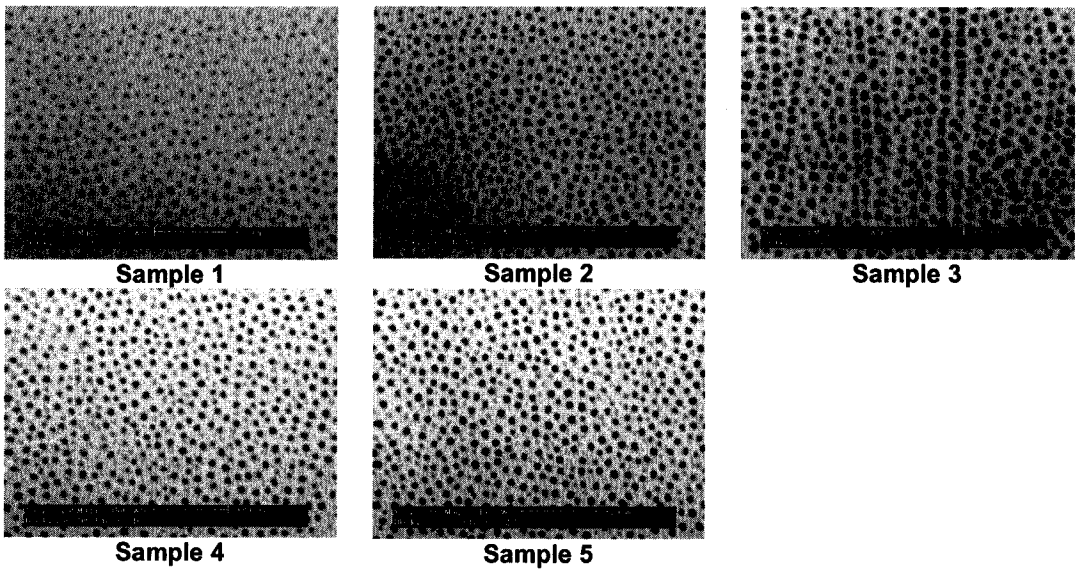

Figure 5.4: Anodized single crystal aluminium samples

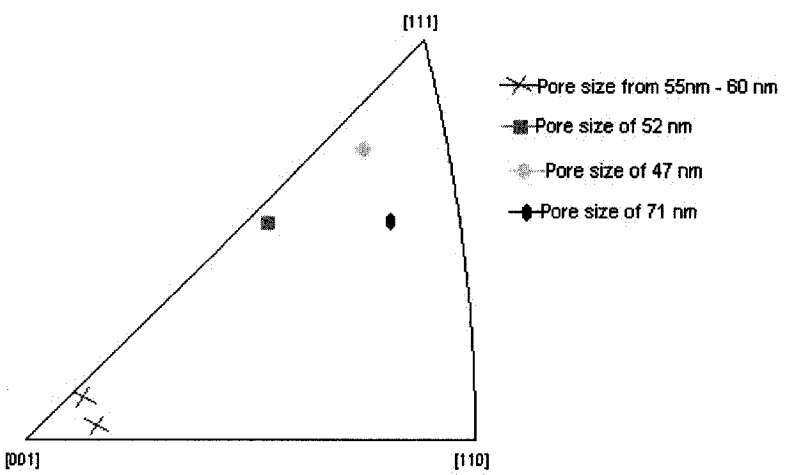

Figure 5.5: Relationship between orientation and pore size given through an inverse pole figure

Table 5.2: Summary of resulting pore sizes on different samples What error +_-_

Sample	Plane (hkl)	Average pore size
1	(235)	47 nm
2	(113)	52 nm
3	(324)	71 nm
4	(001)	56 nm
5	(001)	59 nm

5.3 CONCLUSION

The effects of plane orientation of the substrate on the morphology of anodized alumina were studied by means of macrotexture investigation. The plane orientation of 5 different single crystals was obtained before carrying out an anodizing process. Once anodized, the samples were examined with an SEM, and the pore sizes were measured, and a qualitative observation was done on the uniformity of the pores. Therefore, it can be said that the results were inconclusive. Too few samples were examined in order to come up with a concrete, substantial conclusion. The investigation of anodizing on many more plane orientations would be necessary in order to have a convincing inference.

CHAPTER 6: NICKEL NANOWIRE ELECTRODEPOSTION

Chapter 6 will treat on the synthesis of Nickel nanowires inside the alumina template through the use of a potentiostat. This chapter contains 3 sections; the first one discussing pre-deposition template preparation, the second treating the deposition process and the final chapter assesses the SEM investigation of the deposited nanowires.

6.1 TEMPLATE PREPARATION

Templates where prepared using a 99.998% pure aluminium foil anodized at 40V in a 0.6M oxalic acid electrolyte for a period of 3 to 4 hours with a platinum cathode. Prior to anodizing, the aluminium foil was heat treated at 430^0C for 5 hours in order to create a strong cubic texture. The sample was then eletropolished in a solution of 60% H3PO4 and 40% H_2SO_4. A degreasing step was employed by immersing the sample in acetone for 15 minutes. Anodizing was then carried out under the conditions listed above.

After an anodizing period of 3 hours, the sample was taken out of the anodizing cell and investigated to see if the anodizing treatment had created a through template. This was done by placing the sample in front of a light source, and investigating the transparency of the template. If the template was see-through, the sample was then investigated in the SEM. If no light was visibly coming through the template, the sample was re-anodized under the same conditions for a duration of 1 hour before implementing the pore widening process. After the pore widening process, the sample is then investigated under the SEM. Pore sizes are measured and visual inspection of the uniformity is performed by examining the microscopic images. Templates with average pore sizes larger than 40 nm were deemed acceptable. The back side of the template was also investigated in order to confirm that template was a through-template, and that the barrier layer was removed through the pore widening process.

A gold-palladium layer is then deposited on the back side of the template. The sample is placed in a vacuum chamber, and sputtered with a gold-palladium target for 15 minutes. The sputtering process was first done for periods of 2 to 5 minutes, but resulted unsatisfactory results. The time was increased, reaching a maximum of 15 minutes, which gave suitable results.

6.2 ELECTRODEPOSITION CONDITIONS

Electrodeposition of nickel nanowires was conducted using a Watts bath. The bath was composed of a mixture of 330 g/l $NiSO_4 \cdot 6H_2O$, 45 g/l of $NiCl_2 \cdot 6H_2O$, and 38 g/l H_3BO_3.

In order to achieve proper deposition of nickel inside the nanopores, three important steps were followed carefully. The first step was removing the barrier layer through the pore widening procedure, as explained in the Template Preparation section. The second step was soaking of the template in the electrolyte for a duration of 5 minutes before starting the deposition process. This step was performed to increase the amount of nickel reaching the surface of the Au-Pd substrate in order to ease the deposition process. The third step was employing a high current of 0.02 amperes for a short time of 5 seconds to facilitate uniform nucleation of nickel on the Au layer surface, after which the current was brought back down to 0.01 amperes for the remainder of deposition time, which lasted between 30 seconds to 3 minutes. This process will be referred to as the 2-step deposition process. For one micron thick template, a couple of minutes of soaking time are enough to ensure complete wetting of the bottom of the pores by nickel ions.

Once the deposition is completed, the template is partially dissolved in order to reveal the nanowires which have deposited inside the template. This is done by immersing the template is a 20% NaOH solution for approximately 30 seconds.

6.3 RESULTS AND ANALYSIS

6.3.1 Template Preparation Results

The AuPd coating is a crucial step necessary to successfully accomplishing deposition inside the template. When analysed through energy dispersive spectroscopy, the spectrum indicated counts of the present elements (Al, O, Au and Pd). The reason the oxide layer is

distinguished by EDS is because the coating is thin enough for the x-rays to interact with the oxide below. The carbon count located at the left of the spectrum could be due to impurities on the template, or because of the carbon tape used to secure the template on the SEM sample holder.

It was discovered that a substantially long sputtering time of over 15 minutes was needed to achieve an acceptable coating. Coatings applied for less than 15 minutes yielded templates which were not conducive for deposition. Figure 6.2A and 6.2B show images where after 10 and 15 minutes of sputtering, some areas were only partially coated or even uncoated. Due to the high cost of the AuPd target, sputtering time was limited to a maximum of 15 minutes. Even so, there were still areas with no or poor coverage, as can be seen in figure 6.2A. In some areas, the AuPd target adapted the honeycomb structure of the template, creating nanodot-like structures on the back of the template, as seen in figure 6.4.

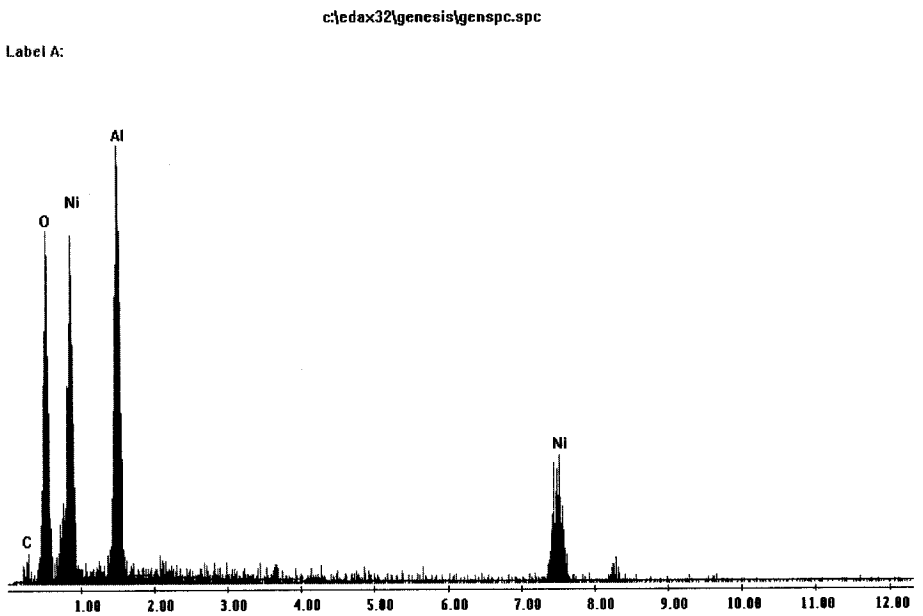

Figure 6.1: Energy dispersive spectrum of AuPd coated template

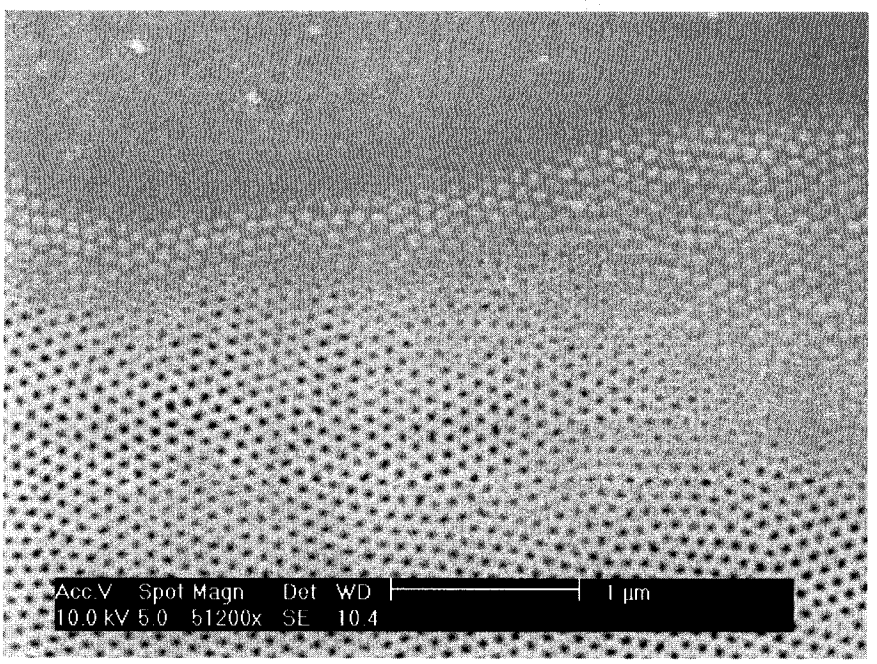

A

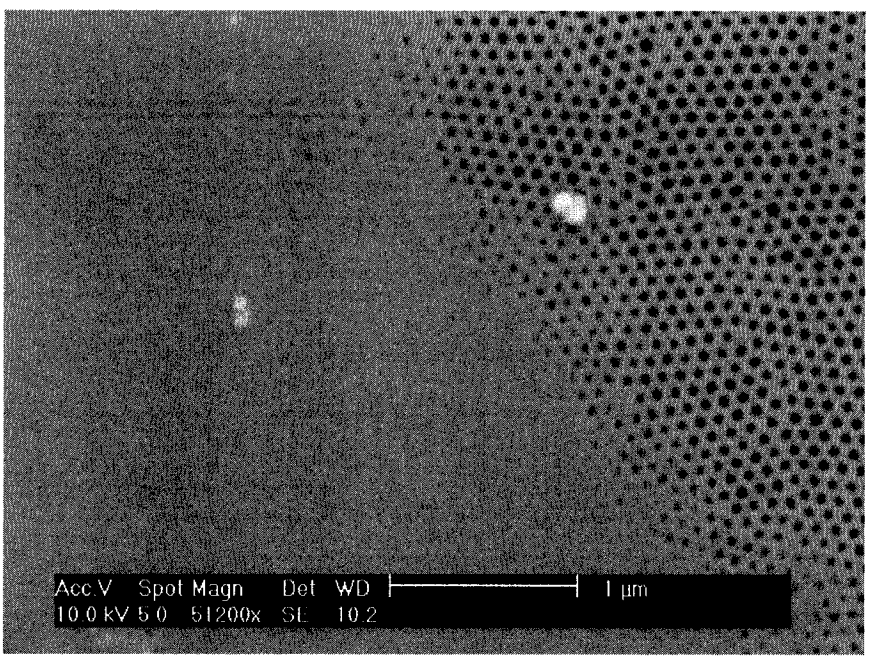

B

Figure 6.2: Area with no AuPd deposition on template after A) 10 and B) 15 minutes sputtering period.

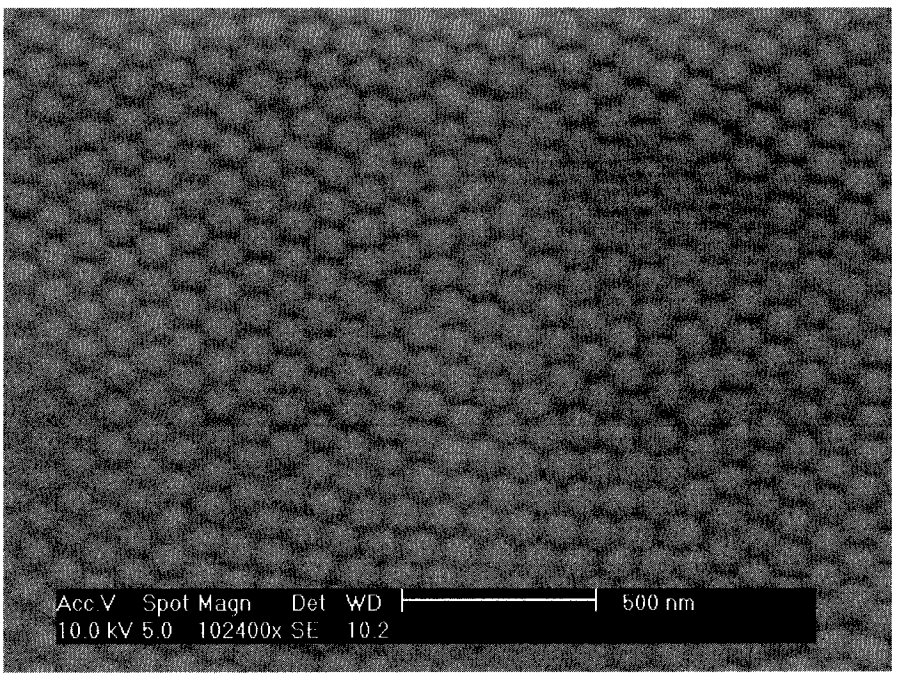

Figure 6.3: Nanodots created by AuPd target on back of template.

6.3.2 Deposition Results and Discussion

The initial deposition processes which yielded negative results where performed without initial soaking of the template in the nickel deposition solution. Deposition times were increased to 200 seconds as seen in figure 6.5, but no deposition was observable. The voltage in this case kept increasing with time, which was indicative of poor or no deposition. When the template was soaked in the nickel solution prior to deposition, nanowires where obtained through the 2-step deposition process after only 50 seconds of deposition time. Figure 6.5 shows a largely increasing potential in the beginning of the deposition subjected to a higher current of 0.02A, and descends to a constant potential of about 1.4V during the second current application of 0.01A.

During deposition, nickel mounted up from the AuPd surface at the bottom of the substrate, and grew inside the pores, building up into nanowires which filled the pores. Figure 6.6 is a SEM image of the nanowires inside a partially dissolved template.

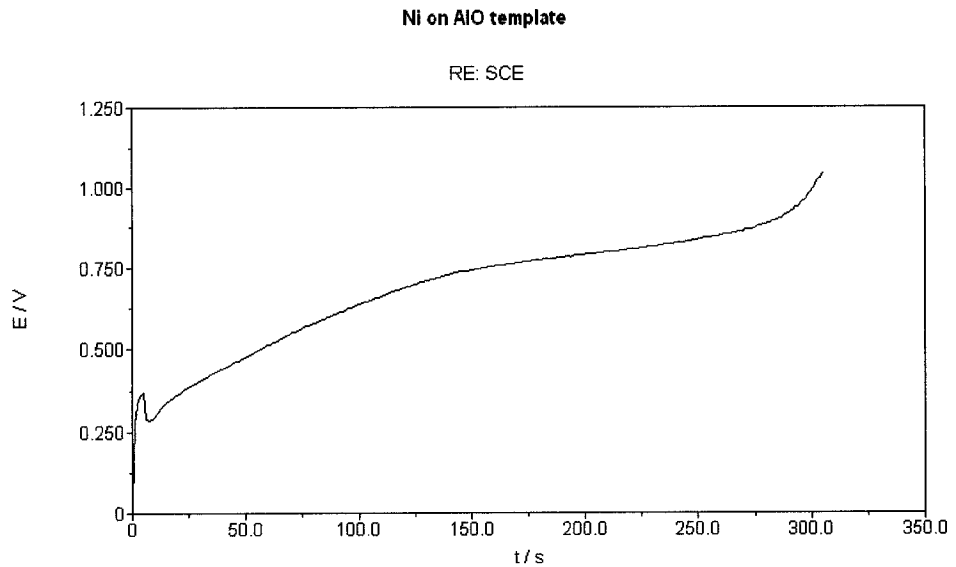

Figure 6.4: Ineffective Ni deposition time.

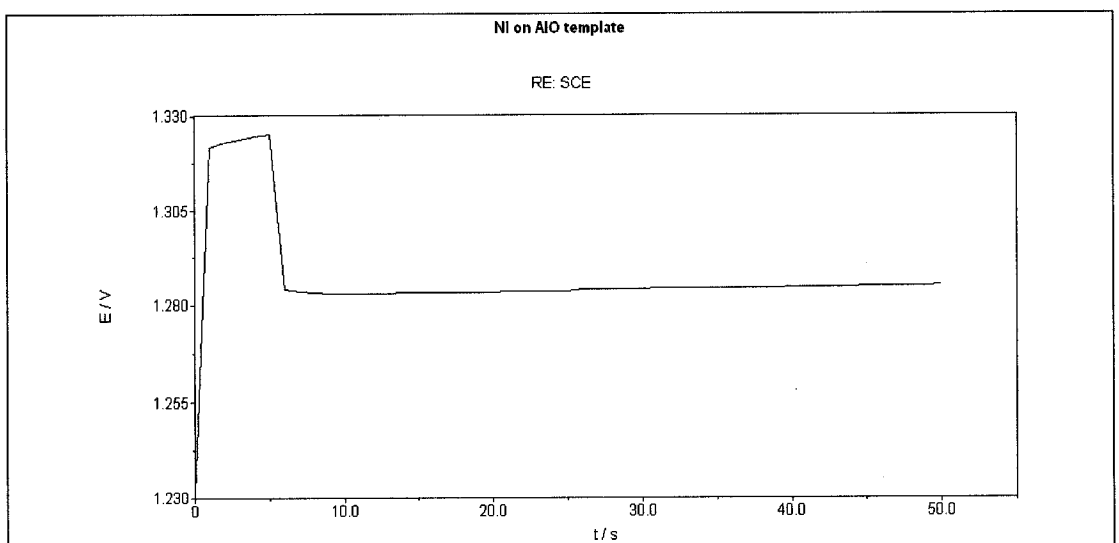

Figure 6.5: Successful Ni deposition time after template soaking

Analysis proved that deposition was not uniform for most experiments. No deposition was obtained on some areas of the template. This is also visible on figure 6.7, which shows an area without any deposited nanowires. One probable reason for the occurrence is a non-uniform coating of the AuPd substrate. It is very probable that during sputtering of the AuPd on the substrate, some regions of the template were not completely covered. This would hinder electrodeposition on those areas due to a lack of electrical contact. Another reason for areas without nanowires could be because the nanowires get washed away during the dissolution of the template and rinsing.

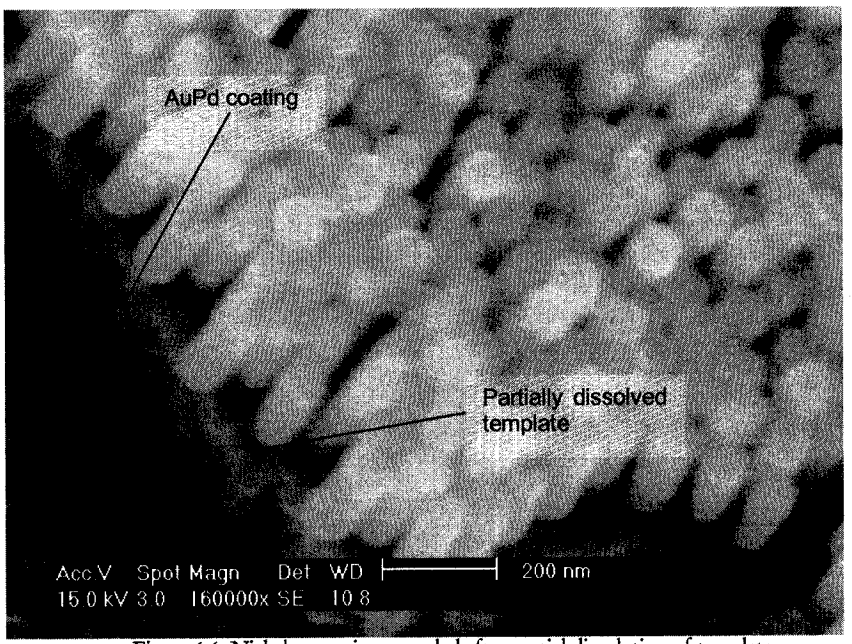

Figure 6.6: Nickel nanowires revealed after partial dissolution of template

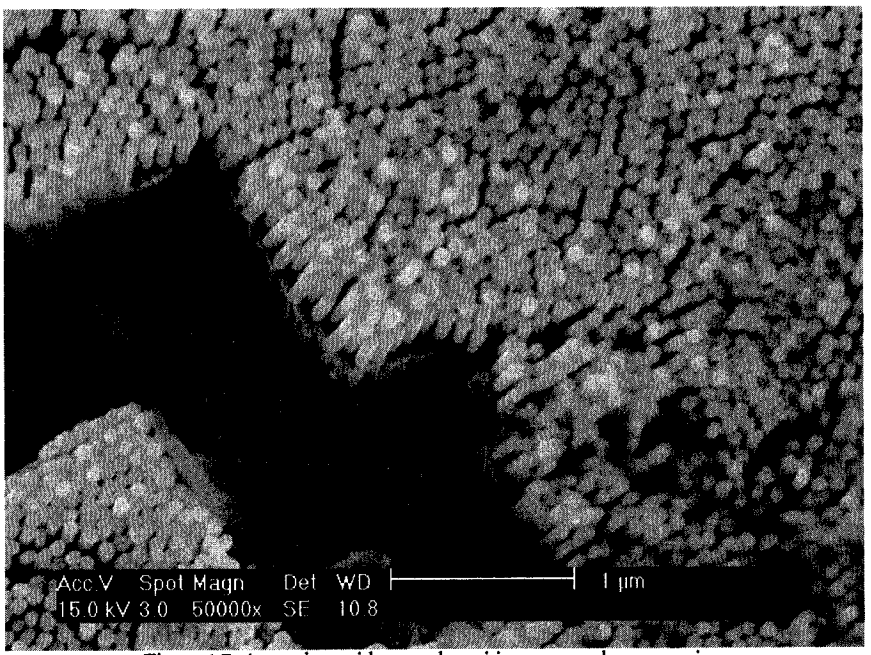

Figure 6.7: Area where either no deposition occurred or nanowires were washed away.

Another important factor which is worth noting is that it is very difficult to handle the template throughout the whole anodizing and electrodeposition process. It is very easy for the template to crack or even brake into small, irrecoverable pieces while manipulating it. Therefore, small cracks may have developed during handling, resulting in areas where sputtering was inconsistent or areas where deposition could not occur.

Following the template dissolution, it was noticeable that the nanowires would attract one another and cluster together, creating different groups of nanowire clusters. This can best be seen in figure 6.8. The areas where the nanowires have clustered together are indicated by the circles.

Nonetheless, there were large areas where deposition was uniform and nanowires where present throughout. This indicates that more thorough nanowire processing is possible

under more vigilant manipulation procedures. Shown in figure 6.9 is a vast area of unvarying presence of nanowires.

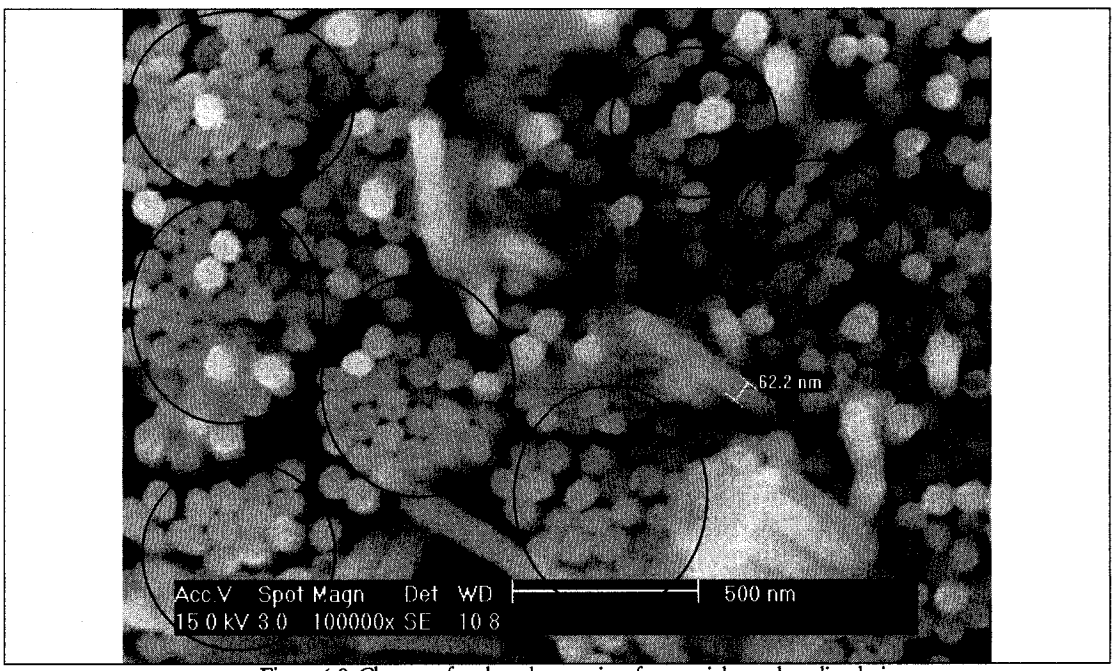

Figure 6.8: Clusters of gathered nanowire after partial template dissolution

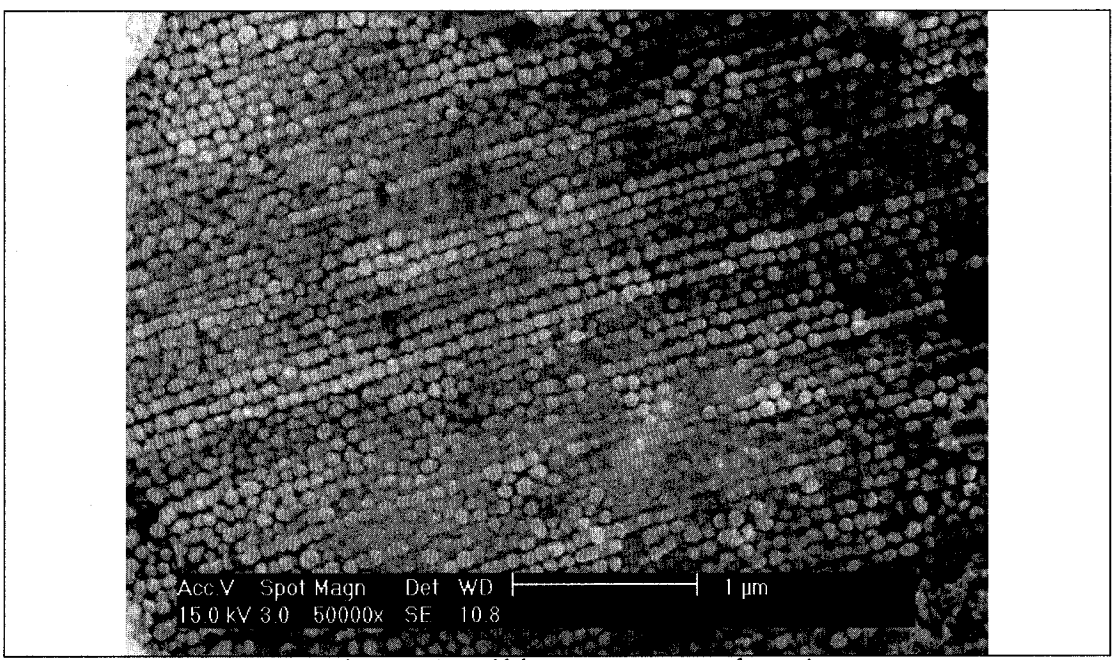

Figure 6.9: Area with homogenous presence of nanowires

6.4 CONCLUSION

Nickel nanowire synthesis was possible via electrodeposition inside an anodized alumina template. Using a 2-step deposition method, electrodeposition inside the through-template was achieved by coating the back of the template with a conductive AuPd layer. There are however, areas where the nanowires have did not deposit, or got washed away after synthesis.

Meticulous care has to be employed during the manipulation of the template in order to keep it flawless and free from cracks away from contamination. Alternate measures have to be implemented to rinse the sample after electrodeposition in order to stop or minimize the removal of nanowires from the template.

CHAPTER 7: SUMMARY, CONCLUSIONS AND FUTURE WORKS

The goal of this project was to investigate the porous formation of anodized alumina, as well as to use it as a template for nanostructure deposition. Anodizing conditions were altered by changing the electrolyte concentration and the type of anode used during anodizing. An attempt was also made to relate texture to the morphology of an anodized template. Nanowires were successfully deposited using electrodeposition inside a through template, using a gold-palladium coating as a conductive support.

The following conclusions can be drawn from the experiments performed during this project.

- When observing anodized alumina templates formed on polycrystalline aluminium samples, grain boundaries distort the order of the pores formed on the sample. The closer the pores come to the boundaries, the smaller and more distorted they become.
- Both 1-step and 2-step anodizing experiments yielded templates with locally ordered arrays of pores. Proceeding with a 1-step anodizing technique leads to less processing time and economy in the materials and energy needed to create porous templates.
- It is possible to fully remove the barrier layer at the bottom of the template while widening the pores of the template. The pores become wider and are clearer when looked at through the SEM. Deposition is also facilitated once the pores are widened.
- The back of the template has a much more uniform appearance than the top of the template. The closely packed honeycomb structure is clear when looked at, and imagery is more vivid at higher magnifications.
- There was no assessed relationship between grain orientation and template morphology. Orientation may have an influence on the morphology of the porous template, but more exhaustive experiments with samples of different orientations need to be preformed.
- Nickel nanowires were created by electrodeposition inside an anodized alumina template. A 2-step deposition method was employed to create them while using a Au-Pd coating on the back of the template as a conductive AuPd base.
- Careful manipulation of the template throughout the experiments is essential due to fragility and extremely brittleness of the through template created on aluminium foil.
- Novel and more efficient ways need to be developed in order to generate templates where nanowires can be successfully created ubiquitously.

The following are suggestions for future work to be done in order to proceed with the work done during this project.

- In order to thoroughly investigate the possibility of an underlying connection between substrate texture and template morphology, single crystal samples with different orientations should be anodized and the results investigated.
- A more efficient and less expensive method of coating the back of the substrate would be beneficial in order to uniformly deposit nanostructures inside anodized alumina templates. The coating should be uniform throughout, covering the entire porous area.
- A better understanding of the formation process of the pores should also be considered. Electrolysis in itself is a complex process where very small alterations can affect the outcome of an experiment. Better understanding the key factors that control the outcome of anodizing is necessary.

REFERENCES

[1] *The Nanotechnology Revolution*, The New Atlantis, # 2,
Adam Keiper, pp. 17-34, Summer 2003.

[2] *Nanotechnology*
Dr. R. Merkle,
www.zyvex.com/nano

[3] *Nanotechnology – What is it?*
Institute of Nanotechnology,
www.nano.org.uk

[4] *Intro. to social and ethical issues in nanotechnology*
B. V. Lewenstein, Cornell Univ.,
HTTP://people.cornell.edu/pages/bvl1/nanoSEI

[5] *For science, nanotechnology poses big unknowns*
R. Weiss, Washington post staff writer,
Washington Post, Sunday Feb. 1, 2004

[6] *Introduction to Electron Beam Lithography*
Henderson Research Group, Georgia Univ.,
HTTP://dot.che.gatech.edu/henderson

[7] *Electron beam lithography in nanoscale fabrication: Recent developments*
A. A. Tseng, K. Cheng, C. D. Chen, K. J. Ma;
IEE Translation on Electronics Packaging Manufacturing, vol.26, #2, April 2003

[8] *Effects of Molecular Weight on Poly(methylmethacrylate) Resolution*
Journal of Vacuum Sci. Tech. vol.14, #1, pp.75-79, 1996

[9] *Anodization of Aluminium: New Applications for a common technology*
C. Hennesthal

Nanotechnology for life science – Nanowizard, JPK Instruments, 2003

[10] *Modern Concepts of Electrochemistry*
A. Despic, V. P. Parkutic, J. O. Bockris, R. E. White,
Pelum Press, NY, pp. 401 1989

[11] *Nanometric Supperlattices: Non-lithographic fabrication, materials, and prospects*
A. Chick, J. M. Xu, Div. Eng. Brown University
Materials Science and Engineering, R43, pp. 103-138 2004

[12] *Anodizing, boundary conditions*
R. S. Alwitt, Northbrook, IL
Dec. 2002
HTTP://electrochem.cwru.edu/ed/encycl/art-a02-anod.htm

[13] *Electrochemically assembled quasi-periodic quantum dot arrays*
S. Bandyopadhyay, A. E. Miller, H. C. Chang, G. Bernerjee, V. Yuzhakov, D. F. Yue, R. E. Ricker, S. Jones, J. A. Eastman
Nanotechnology 7 pp. 360-371 1996

[14] *Structural features of crystalline anodic alumina films*
H. Uchi, T. Kanno, R. S. Alwitt
Journal of Electrochemical Society, vol. 148, pp.B17-B23, 2001

[15] *Conditions of fabrication of ideally ordered anodic porous alumina using pretextured aluminium*
H. A. Soh, K. Nishio, M. Nakao, T. Tamamura, H. Masuda
Journal of Electrochemical Society, vol. 148, pp. B152-156, 2001

[16] *The surface treatment of finishing of aluminium and its alloys*
S. Wernick, R. Pinner, P. G. Sheasby
ASM internaltional, 1987, Metals Park, OH

[17] *Crystalline aluminium oxide films*
R. S. Alwitt, H. Takei
Thin Films Science and Technology, vol.4, pp.741-746, 1983

[18] *Anodic films on aluminium*
G. E. Thompson, G. C. Woods
Treatise on Materials Science and Technology, vol23, pp.205-329 1983

[19] *Self organized formation of hexagonal pore arrays in anodic alumina*
O. Jessensky, F. Muller, U. Gosele,
Applied Physics Letters, vol.10, pp.1173-1175, 1998

[20] *Hexagonal pore arrays with 50-420 nm interpore distance by self-ordering*
A.P. Li, F. Muller, A. Birner, K. Nielsch, U. Gosele,
Journal of Applied Physics, vol. 84, #11, pp. 6023, 1998

[21] *Self ordered regimes of porous alumina*
K. Nielsch, J. Choi, K. Schwirn, R. B. Wehrspohn, U. Gosele
Nanoletters, vol.2, #7, pp.677-688, 2002

[22] *Carbon nanotubes with triangular cross-section fabricated using anodic porous alumina as the template*
T. Yanagishita, M. Susaki, K. Nishio, H. Masuda, Advanced Materials, vol.16, #5, pp 429-422, 2004

[23] *Self-organized formation of hexagonal pore structures in anodic alumina*
O. Jessensky, F. Muller, U. Goselle
Journal of the Electrochemical Society, vol. 145, #11, pp. 3735-3740, 1998

[24] *Ordered metal nanohole arrays made by a two-step replication of honeycomb structures of anodic alumina*
H. Masuda, K. Fukuda
Science, vol. 268, #5216, pp. 1466, 1995

[25] *Arrays of ZnO nanowires fabricated by a simple chemical solution route*
H. Zhang, X. Ma, J. Xu, J. Niu, D. Yang
Nanotechnology, vol.14, pp. 423-426 2003

[26] *Poly(ethylene glycol) grafted nanoporous alumina membranes*
K. Popat, G. Mor, G. Grimes, T. A. Desai
Journal of membrane science vol.243, pp.97-106, 2004

[27] *Electroplating*
M. Schlesinger, Dept. of physics, Univ. of Windsor (ON)
Electrochemistry Encyclopaedia, 2002,
www.electrochem.cwru.edu

[28] *Handbook of chemical vapor deposition: Principles, technology, and applications (2nd edition)*
H. O. Pierson
W. Andrew publishing/ Noyes, pp. 345-349, 1999

[29] *Fabrication of highly ordered metallic nanowire arrays by electrodeposition*
A. J. Yin, J. Li, W. Jian, A. J. Bennett, J. M. Xu
Applied Physics Letters, Vol. 79, #7, pp. 1039-1041, 2001

[30] *Science behind the news: Understanding nanodevices*
National Cancer Institute web site:
http://press2.nci.nih.gov/sciencebehind/nanotech/nano12.htm

[31] V. *Introduction to Texture Analysis: Macrostructure, Microstructure and Orientation mapping*
V. Randle, O. Engler, pp. 59-121, CRC Press, 2000

[32] *Microtexture determination and its applications*
V. Randle, pp. 128-151, 2nd edition, Maney Publishing, 2003

[33] www.ebsd.com/textureanalysis.htm

[34] http://media.wiley.com/product_data

[35] *Texture and microstructure in polycrystalline materials*

J.A. Szpunar

Spring 2006 Texture and Microstructure in Polycrystalline Materials course notes.
McGill University. Montreal, Canada.

[36]*Conditions of fabrication of ideally ordered anodic porous alumina using pretextured aluminium*

H. A. Soh, K. Nishio, M. Nakao, T. Tamamura, H. Masuda
Journal of Electrochemical Society, vol. 148, pp. B152-156, 2001

[37] *Hexagonal pore arrays with 50-420 nm interpore distance by self-ordering*
A.P. Li, F. Muller, A. Birner, K. Nielsch, U. Gosele,
Journal of Applied Physics, vol. 84, #11, pp. 6023, 1998

[38] *Direct electrodeposition of highly ordered magnetic nickel nanowires on silicon wafer*
S. Wen, J.A. Szpunar,
Micro & Nano Letters, vol. 1, #2, p 89-93,1 Dec. 2006

[39] *Ordered Ni nanowire tip arrays sticking out of the anodic alumina oxide template*
G. Meng, A. Cao, J.Chen, A. Vijayaraghavan, Y. Jung, M. Shima, P. Ajayan
Journal of Applied Physics 97, #6, pp. 064303, 2005

[40] *Fabrication of alumina nanotubes and nanowires by etching porous alumina membranes.*
Z. Xiao, C. Han, U. Welp, W. Kwok, G. Willing, J. Hiller, R. Cook, D. Miller, G. Crabtree
Nano Letters vol. 2, #11, pp. 1293-1297, 2002.

[41] *Porous alumina template based nanodevices*
K. Jain, S. Lakshmikumar
IETE Technical Review, Vol.19, #5, pp. 293-306, 2002

[42] *Metal nanostructures prepared by template electrodeposition*
W. Schwarzacher, O. Kasyutich, P. Evans, M. Darbyshire, G. Yi, V. Fedosyuk, F. Rousseaux, E.Cambril, D. Decanini
Journal of Magnetism and Magnetic Materials, 198-199, pp. 185-190, 1999

[43] *Arrays of Ni nanowires in alumina membranes: magnetic properties and spatial ordering.*
M. Vasquez, M. Hernandez-Velez, K. Pirota, A. Asenjo, D. Navas, J. Velazquez, P. Vargas
European Physical Journal B 40, pp. 489-497, 2004